Ecole Polytechnique Fédérale de Lausanne

Photon polarization sensitivity in $B_s^0 \to \phi\gamma$ decays at LHCb

January 17, 2014

Eleonie van Schreven

Professor: O. Schneider
Supervisor: A. Puig

Contents

1 Introduction

The Standard Model (SM) of particle physics formulated up to 1970s was experimentally tested all along the next 40 years, with as most recent evidence the discovery of the Higgs boson [19][20]. Nevertheless open questions not answered by this model still remain, such as the origin of dark matter and dark energy, the oscillations of the neutrinos or the asymmetry between matter and antimatter. New Physics (NP) models which try to fill this gap are either extensions of the SM or totally new theories. The search for experimental confirmation of such models can be done directly or indirectly: the direct method consists in observing a particle predicted by a Beyond the SM theory, whereas indirect methods investigate quantities predicted both by the SM and the new model but with different values. The research done at LHCb (CERN) is mainly indirect measurement of NP.

The photon polarization in radiative B meson decays is predicted at very different values depending on the model and as such presents an interesting null test of the SM. It is defined by:

$$\lambda_\gamma = \frac{|A_R|^2 - |A_L|^2}{|A_R|^2 + |A_L|^2}, \tag{1}$$

where $A_L(A_R)$ are the decay amplitude of the left (right) handed photons in these kind of decays.

This report will focus on the study of the photon polarization $B_S^0 \to \phi\gamma$ decays at the LHCb experiment. This is one of the key measurement to be performed by the LHCb experiment [8]. Firstly, the theoretical background as well as the motivation behind the choice of the decay will be exposed. We will then go on to generate Monte Carlo toy events that will allow us to investigate the different contribution to the sensitivity of the measurement by adding experimental effect such as acceptance, resolution or uncertainty on certain parameters.

To main goal is to asse the sensitivity of measuring the photon polarization with the data collected by LHCb in the Run1 of LHC (2011 and 2012) and to determine the capacity of the LHCb experiment to rule out theories BSM.

2 Motivation

Flavor Changing Neutral Current weak interactions can only happen through loop diagram in the SM. New heavy particles circulating in such loops can modify the physics observables allowing the study of NP phenomena at large

energy scales. An example of such quantities is the photon polarization. The Feynman diagram for $b \to s\gamma$ transitions is shown in Fig.1. The V-A coupling of the $W^{\pm}$ bosons does not restrict the polarization of the photon but highly suppresses one of the final states; the W boson primarily couples to the left-handed quarks [8], [21], resulting in mainly left-handed photons. The transition $b \to s\gamma$ is given, without the QCD corrections, by [21]:

$$\bar{s}\Gamma(b \to s\gamma)_\mu b = \frac{e}{(4\pi)^2}\frac{g^2}{2M_W^2}V_{ts}^* V_{tb} F_2 \bar{s} i\sigma_{\mu\nu}(p_b - p_s)^\nu \left(m_b \frac{1+\gamma_5}{2} + m_s \frac{1-\gamma_5}{2}\right) \tag{2}$$

where:

- $p_{b,s}$ is the four-momentum of the b and s quarks
- F_2 is the loop function

The helicity amplitude can be computed and one finds that only the first (second) term remains when multiplying Eq. 2 by the left-handed (right-handed) polarization vector [21]. This translates into the fact that the ratio A_R/A_L scales as the mass ratio $m_s/m_b \approx 0.02$ hence explaining the predominance of left-handed photons in the SM [8], [21].

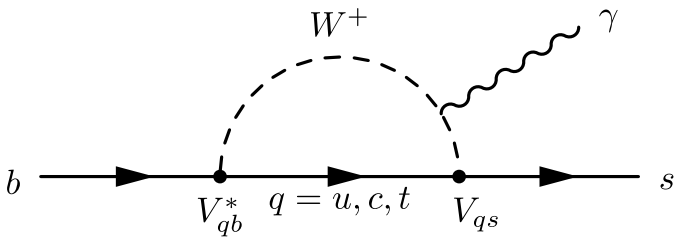

Figure 1: Feynman diagram for $b \to s\gamma$

However NP models such as the Left-Right Symmetric Model (LRSM, [18]) or the unconstrained Minimal Supersymmetric Standard Model (uMSSM, [16], [17]) predict a larger fraction of right-handed photons. In the LRSM this is due to a chirality flip along the heavy t-quark line in the loop whereas for the uMSSM it is due to a chirality flip along the gluino line.

3 Time-dependent decay rate of B mesons

The time dependent decay rate of a B meson going to a photon and a CP eigenstate ($B \to f_{CP}\gamma$) can be written as:

$$\Gamma_{B(\bar{B})}(t) \sim |A|^2 e^{-\Gamma t}\left(\cosh(\frac{\Delta\Gamma t}{2}) - \mathcal{A}^{\Delta}\sinh(\frac{\Delta\Gamma t}{2}) \pm \mathcal{C}\cos(\Delta m t) \mp \mathcal{S}\sin(\Delta m)\right), \tag{3}$$

with

$$\mathcal{C} = \frac{(|A_L|^2 + |A_R|^2) - (|\bar{A}_L|^2 + |\bar{A}_R|^2)}{|A_L|^2 + |A_R|^2 + |\bar{A}_L|^2 + |\bar{A}_R|^2} \tag{4}$$

$$\mathcal{S} = \frac{2\Im\left(\frac{q}{p}(\bar{A}_L A_L^* + \bar{A}_R A_R^*)\right)}{|A_L|^2 + |A_R|^2 + |\bar{A}_L|^2 + |\bar{A}_R|^2} \tag{5}$$

$$\mathcal{A}^{\Delta} = \sin(2\psi)\cos(\phi) \tag{6}$$

$$\tan\psi = \frac{\bar{B} \to f_{CP}\gamma_R}{\bar{B} \to f_{CP}\gamma_L}, \tag{7}$$

where

- Γ is the width of the B decay,
- $\Delta\Gamma$ is the width difference between two eigenstates in the B mesons system,
- $A_{L,R}$ are the amplitudes of emission of left-handed and right-handed photons respectively in B decays ($A_{L,R} = A(B \to f_{CP}\gamma_{L,R})$),
- $\bar{A}_{L,R}$ are the amplitude of emission of left-handed and right-handed photons respectively in $\bar{B}$ decays ($\bar{A}_{L,R} = A(\bar{B} \to f_{CP}\gamma_{L,R})$,
- ϕ is the B mixing phase,
- ψ relates to the ratio of right-handed or left-handed photons in B or $\bar{B}$ decays (Eq. 7),
- Δm is the mass difference between the two eigenstates in the B system.
- T physically allowed range of values of $\mathcal{A}^{\Delta}$ is between -1 and 1 [8].

The sign of the cos and sin terms is fixed by choosing to study either the particle B or the antiparticle $\bar{B}$. Therefore the term $\mathcal{S}$ will only appear in the difference of time dependent decay rates between B and $\bar{B}$ whereas $\mathcal{A}^{\Delta}$ will appear in the sum. This makes $\mathcal{A}^{\Delta}$ the ideal parameter to study the photon polarization.Since the analysis can be performed without the need

of tagging; this considerably increases our efficiency. Hence we choose to study an untagged decay, measuring the parameter $\mathcal{A}^{\Delta}$.

In order to choose which specific decay to observe let us notice that $\mathcal{A}^{\Delta}$ is sensitive to $\Delta\Gamma$. The measurement of $\mathcal{A}^{\Delta}$ will be facilitated for high values of $\Delta\Gamma$ and therefore, from the value in Table 1 the B_s system is a suitable candidate for this study.

Parameter	B_s^0	B^0
τ_s	(1.516 ± 0.011) ps	1.519 ± 0.007
$\Delta\Gamma_s$	(0.081 ± 0.011) ps^{-1}	< 0.12 at CL=95%

Table 1: B meson properties [5]

Summarizing the time dependent decay rate for a non-tagged study of $B_S^0 \to \phi\gamma$ is:

$$\Gamma_{B_s}(t) \sim e^{-\Gamma_s t}\left(\cosh(\frac{\Delta\Gamma_s t}{2}) - \mathcal{A}^{\Delta}\sinh(\frac{\Delta\Gamma_s t}{2})\right) \tag{8}$$

Figure 2 shows the time dependent decay rate for two different values of $\mathcal{A}^{\Delta}$: the SM value ($\mathcal{A}^{\Delta} = 0.045$ [14][1]) and $\mathcal{A}^{\Delta}$ =1 which considerably differs from the SM prediction.

These two models have very different values of $\mathcal{A}^{\Delta}$ and should thus be easier to distinguish, but as can be seen on Fig.2 the decay rates are very close and can be distinguished mainly in the tails of the distributions. Therefore the main contribution to the measurement of $\mathcal{A}^{\Delta}$ comes from decay rate at high proper times.

Equation 8 can be expanded as following:

$$\Gamma_{B_s}(t) \sim \frac{|A|^2}{2}\left((1-\mathcal{A}^{\Delta})e^{-(\Gamma_s - \Delta\Gamma_s/2)t} + (1+\mathcal{A}^{\Delta})e^{-(\Gamma_s+\Delta\Gamma_s/2)t}\right) \tag{9}$$

For small values of $\epsilon = \frac{\Delta\Gamma_s}{2}t$, Eq.8 can be rewritten as:

$$\Gamma_{B_s}(t) \sim |A|^2 e^{-\Gamma_s t}\left(1 - \mathcal{A}^{\Delta}\frac{\Delta\Gamma_s}{2}t + \frac{1}{2}\left(\frac{\Delta\Gamma_s t}{2}\right)^2 + \mathcal{O}\left(\left(\frac{\Delta\Gamma_s}{2}t\right)^3\right)\right)$$
$$\Rightarrow \Gamma_{B_s}(t) \sim |A|^2 e^{-\Gamma_{B_s\to\phi\gamma}t} \tag{10}$$

[1]The value cited in [14] is 0.047. A typo was made at the beginning of this project and only discovered too late to redo all the toys. We will show further that this has a negligible effect

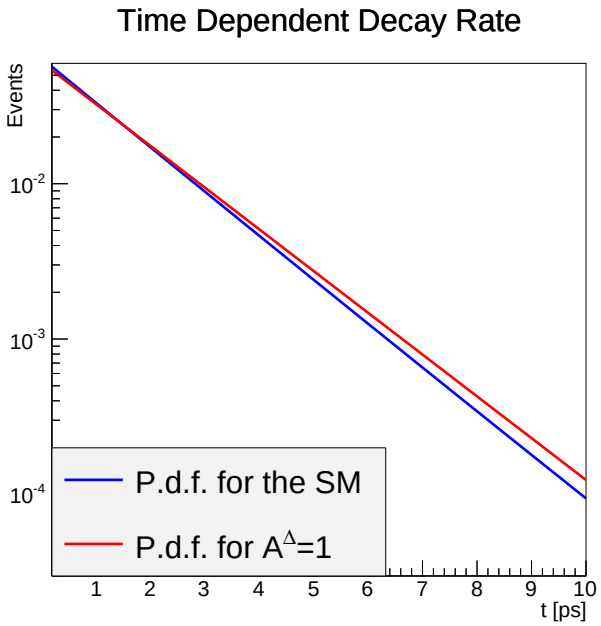

Figure 2: Time-dependent decay rate for $B_S^0 \to \phi\gamma$

where

$$\Gamma_{B_s \to \phi\gamma} = \Gamma_s + \mathcal{A}^{\Delta} \frac{\Delta\Gamma_s}{2}, \tag{11}$$

is the effective lifetime of the B_s meson in $B_s \to \phi\gamma$. Equation 10 was obtained by keeping only the linear terms, and thus is valid only for small $\mathcal{A}^{\Delta}$. In addition it is only valid for small values of ϵ compared to Γ_s which is clearly not the case in the range [0,10] ps. For instance at 10 ps, $\epsilon = 0.405$ ps^{-1} which cannot be considered small compared to $\Gamma_s = \frac{1}{\tau_s} = 0.65$ ps^{-1}.

Let us study further this approximation in order to investigate its goodness. If we fix τ_s and $\Delta\Gamma_s$, the two remaining parameters that can be varied are $\mathcal{A}^{\Delta}$ and the upper limit of the proper time range.

To better understand the effect of using the approximation of Eq. 10, it is very instructive to study the ratio between the nominal decay rate from Eq. 8. Figure 3, generated with $A^{\Delta} = 0.045$ shows how the approximation diverges up to 10% for values of t close to 10 ps. One can then modify the value of A^{Δ} in the approximation to try to make the ratio as close as possible to 1 and study the difference with respect to the input value of 0.045. More precisely, we find the $A^{\Delta\prime}$ that causes the integral of the ratio to be 1 in the chosen t interval. In the case of $t \in [0, 10]$ ps, the value is $A^{\Delta\prime} = -0.1766$, and therefore the induced bias is 0.22 ps, quite large considering that previous studies estimate the sensitivity to A^{Δ} to be ~ 0.2.

This study can then be repeated by varying the upper limit of the studied t range, and the obtained values of $A^{\Delta\prime}$ are shown in Fig. 4. This result confirms that the approximation of Eq. 10 cannot be used in this analysis, since the expected range to be used is $[0, 10]$ ps; the approximation is valid, at best, between 0 and 1 ps. It is worth noting that this approximation was presented as valid for all t in multiple sources, such as [9], [12] and [15]. However, it will not be used in this document for the mentioned reasons.

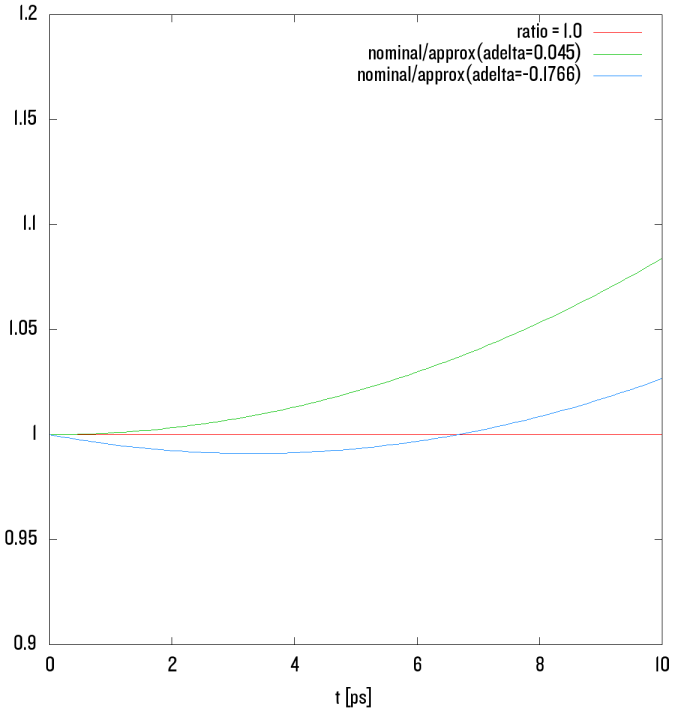

Figure 3: Ratio of the full p.d.f described by Eq. 8 over the approximation 10 for different values of input $\mathcal{A}^{\Delta}$

4 Pure MonteCarlo toys

The main goal of the study is to retrieve the parameter $\mathcal{A}^{\Delta}$ and to study its uncertainties induced by different experimental effects. In order to do this we want to fit the time dependent decay rate for $B_S^0 \to \phi\gamma$ according to Eq. 8.

Let us start by defining our pure Monte Carlo toys, for which the procedure is the following:

1. Generate a data set of N_{ev} events using as p.d.f. Eq. 8 with a fixed value of $\mathcal{A}^{\Delta}$ depending on the model and proper time value between 0 and 10 ps.

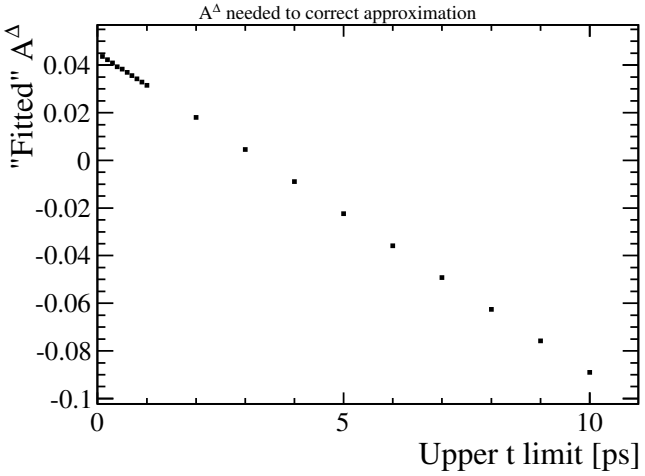

Figure 4: Fitted value of $\mathcal{A}^{\Delta}$ as a function of the upper limit of proper time used in the approximation 10

2. Perform an unbinned maximum likelihood fit with the $\mathcal{A}^{\Delta}$ parameter free.

3. Retrieve the fitted value of $\mathcal{A}^{\Delta}$.

4. Iterate this N_{toy} times and retrieve $\mathcal{A}^{\Delta}$ for each of the created data set (toy).

5. Plot the distribution of $\mathcal{A}^{\Delta}$ and fit it with a gaussian. The mean of this gaussian is the central value of $\mathcal{A}^{\Delta}$ and its width is the statistical error of $\mathcal{A}^{\Delta}$.

6. Compute the pull of $\mathcal{A}^{\Delta}$ using

$$g = \frac{\mathcal{A}^{\Delta}_{\text{fit}} - \mathcal{A}^{\Delta}_{\text{true}}}{\sigma_{\text{fit}}}, \tag{12}$$

   where $\mathcal{A}^{\Delta}_{\text{fit}}$ are the fitted values of $\mathcal{A}^{\Delta}$, $\mathcal{A}^{\Delta}_{\text{true}}$ is the initial value entered in the generating p.d.f. and σ_{fit} is the statistical error of $\mathcal{A}^{\Delta}_{\text{fit}}$ meaning the width of the gaussian distribution of $\mathcal{A}^{\Delta}_{\text{fit}}$.

We expect the pull described in Eq. 12 to be distributed as a gaussian of mean 0 and width 1 [4].
We use `RooBDecay` to create the p.d.f. according to Eq. 8 and `RooMCStudy` to generate the toys and do a Maximum Likelihood unbinned fit.

Results for these simulations are shown in Fig. 5 (6) for $\mathcal{A}^{\Delta} = 0.045$, $N_{\text{ev}} = 900$ and $N_{\text{toy}} = 10000$ ($N_{\text{ev}} = 3000$, $N_{\text{toy}} = 50000$).
As explained in earlier, the pull should have a mean of 0 and a width of

1. The mean of 0 is a sign of an unbiased estimator whereas a width of 1 indicates that the errors were computed correctly. One can see from the pulls on Fig. 5 and 6 that the fits are slightly biased as the means are not null. The fitted $\mathcal{A}^{\Delta}$ underestimates the true value. This bias will be investigated in further sections.
Finally let us notice that at low N_{ev}, the distributions are not fully gaussian, an this could influence the pulls. This is probably due to the fact that we are not in the asymptotic regime.

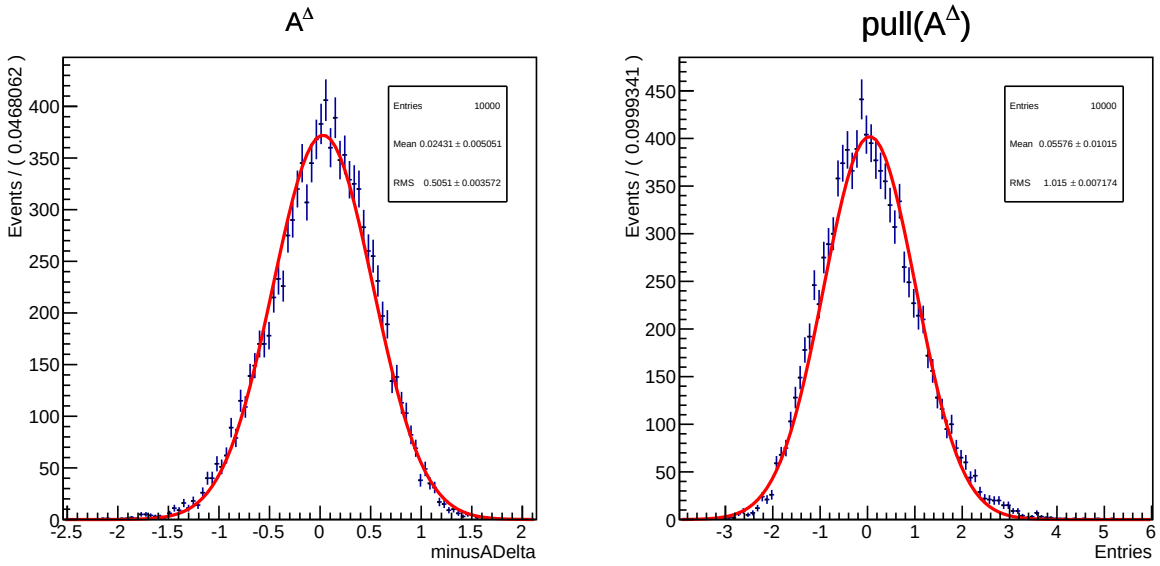

Figure 5: $\mathcal{A}^{\Delta}$ and pull($\mathcal{A}^{\Delta}$) for pure toys with 900 events and 10000 toys in the SM

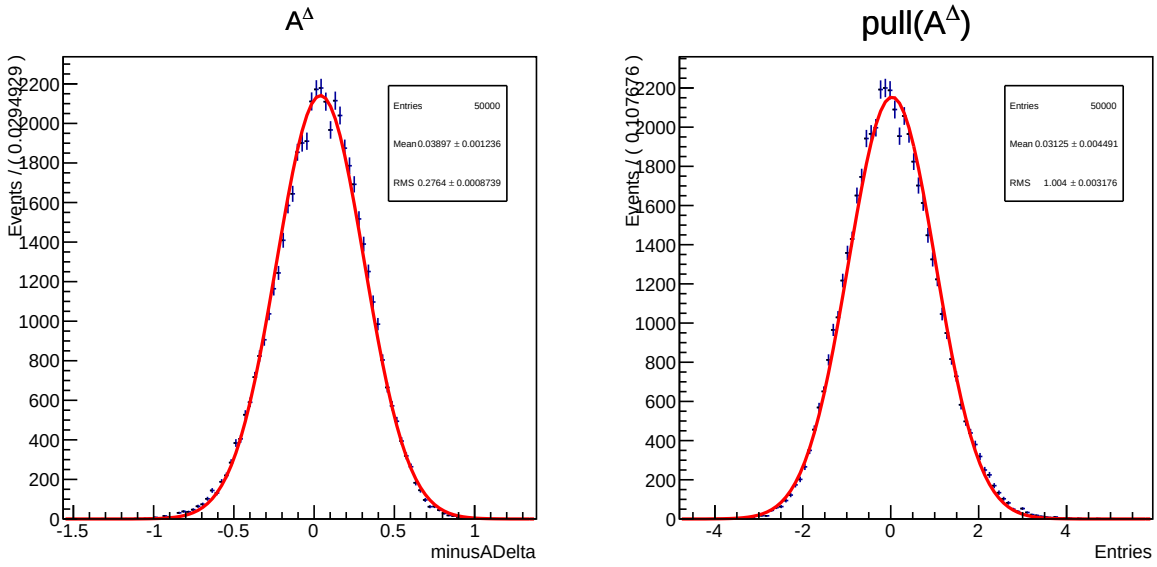

Figure 6: $\mathcal{A}^{\Delta}$ and pull($\mathcal{A}^{\Delta}$) for pure toys with 3000 events and 50000 toys in the SM

It is important, before analyzing this bias, to study the scaling of the statistical uncertainty of $\mathcal{A}^{\Delta}$ as a function of N_{ev}.

4.1 Statistical uncertainty

In order to study the purely statistical uncertainty, we generate several sets of toys varying the number of events per toys, from 900 events to 100000 events always keeping $N_{\text{toy}} = 10000$.
For each set of toys we fit a gaussian to the distribution of $\mathcal{A}^{\Delta}$ values. In Fig. 7 one can see the standard deviation $\sigma_{\mathcal{A}^{\Delta}}$ of these gaussian as a function of the number of events. The green curve represents a fit of the form $p_0 + \frac{p_1}{\sqrt{N}}$ which its results summarized in Table 2. As expected the statistical error on $\mathcal{A}^{\Delta}$ scales approximately as $1/\sqrt{N}$.

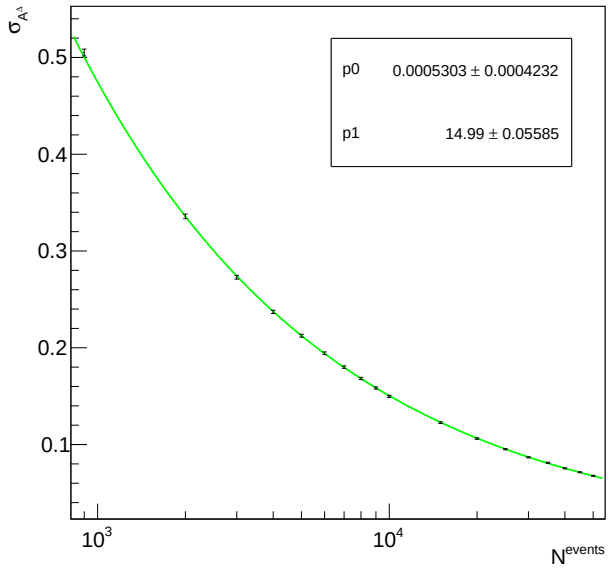

Figure 7: Statistical error for pure toys depending on N_{ev} the number of events and 10000 toys

Parameter	**Value**
p_0	$(5.3 \pm 4.2) \times 10^{-4}$ s
p_1	(14.99 ± 0.05)

Table 2: Fit results for the statistical error depending on N_{ev}

We can also study the expected statistical sensitivity on $\mathcal{A}^\Delta$ as a function of its value. In Fig. 8. we can see that the sensitivity increases for high values of $\mathcal{A}^\Delta$ [2].

[2]Let us also notice that the sensitivities at $\mathcal{A}^\Delta$=0.045 and $\mathcal{A}^\Delta$=0.047 are essentially the same, thus our typo in the values of the SM $\mathcal{A}^\Delta$ will have a negligible on the study. If we use the fit to compute the uncertainties, we get $\sigma_{\mathcal{A}^\Delta}(0.045) = 0.3080$ and $\sigma_{\mathcal{A}^\Delta}(0.047) = 0.3079$

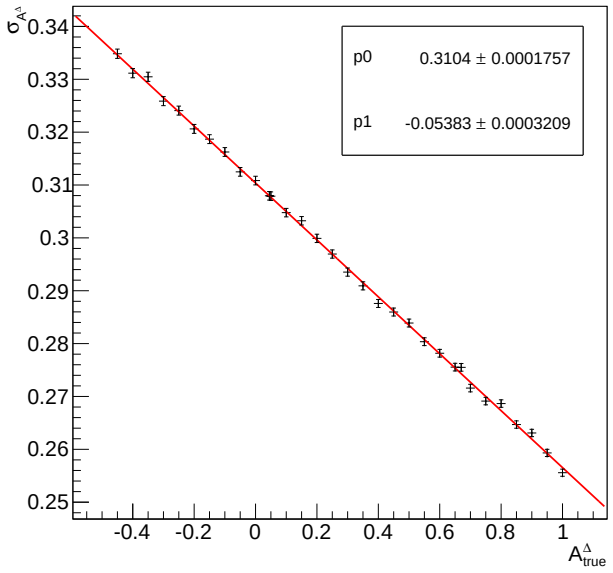

Figure 8: $\sigma_{\mathcal{A}^\Delta}$ as a function of $\mathcal{A}^\Delta$ for $N_{\text{ev}} = 3000$ and $N_{\text{toy}} = 50000$

4.2 Bias

In order to understand the bias observed in the data we start by generating toys with different number of events to study the evolution of this bias. Figure 9 shows the results for this study and one can note that the bias seems to disappear for high number of events, explaining why it was not observed in other studies using higher statistics ([9] [12]). As the bias seems to disappear at large N_{ev} it is likely related to the limited amount of data available.
The Maximum Likelihood Estimators (MLE) used in data fitting are built as a function of the data points and have the following main properties :

- Consistent: the estimator is unbiased for large number of events
- Efficient: the variance of the estimator is minimal at large number of events.
- Asymptotically normal: as the sample statistics increases, the distribution of the MLE tends to a gaussian distribution with mean equal to the true value.

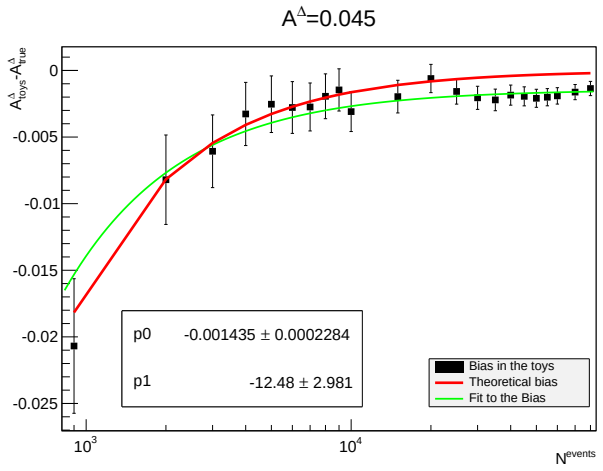

Figure 9: Bias for pure toys depending on N the number of events and 10000 toys

An estimator is said to be unbiased if its expectation value is equal to the true value for all N_{ev}. However, this property is not guaranteed, and as shown in Fig. 9 our fit does not present it. The bias induced by the MLE for the full time-dependent decay rate (Eq. 8) can not be computed analytically, but this can be done for the approximation Eq. 10. Let us keep in mind that this approximation is valid only for small values of proper time, but it is useful to gain a better intuition of the possible statistical bias. The MLE of an exponential distribution can be biased. In fact the MLE for $\frac{1}{\tau}e^{(1/\tau)t}$ is unbiased whereas $\Gamma e^{\Gamma t}$ is biased. The choice of the estimator could thus be a reasonable explanation for our bias.

The MLE and its bias are found in the case of the exponential approximation in the following way.

$$L = \prod_{i=1}^{N} \Gamma_{B_s}(t_i) = \left(\Gamma_s + \frac{\mathcal{A}^{\Delta}\Delta\Gamma_s}{2}\right)^N \exp\left(-\left(\Gamma_s + \frac{\mathcal{A}^{\Delta}\Delta\Gamma_s}{2}\right)\sum_{i=1}^{N} t_i\right) \quad (13)$$

Therefore:

$$\ln L = N \ln\left(\Gamma_s + \frac{\mathcal{A}^{\Delta}\Delta\Gamma_s}{2}\right) - \left(\Gamma_s + \frac{\mathcal{A}^{\Delta}\Delta\Gamma_s}{2}\right)\sum_{i=1}^{N} t_i \quad (14)$$

As the MLE maximizes the likelihood, $\frac{\partial \ln L}{\partial \mathcal{A}^{\Delta}}(\hat{\mathcal{A}}^{\Delta}) = 0$. Hence:

$$\hat{\mathcal{A}}^{\Delta} = \frac{2}{\Delta\Gamma_s}\left(\frac{N}{\sum_{i=1}^{N} t_i} - \Gamma_s\right). \quad (15)$$

If we use the results of appendix A we find that this estimator is biased meaning that $\mathbb{E}(\hat{\beta}) \neq \beta$, and the bias is:

$$b_{\mathcal{A}^\Delta} = \frac{\mathcal{A}^\Delta}{N-1} + \frac{2\Gamma_s}{\Delta\Gamma_s(N-1)} \tag{16}$$

One should keep in mind that this bias is valid at best for times between 0 and 1 ps and not between 0 and 10 ps as studied here. This calculation still gives us an indication on the nature of the observed bias.
Figure **??** show this theoretical bias as a function of the number of events for the SM, whereas Fig. 9 shows the observed bias also for the SM, and for $N_{\text{toy}} = 10000$. The curve shown on Fig. 9 is the function $p_0 + p_1/N$ fitted to the data. As the exponential approximations not valid, the bias will need to be determined experimentally.

Bias as a function of $\mathcal{A}^\Delta$ Let us study the dependence of the bias on $\mathcal{A}^\Delta$ for a fixed $N_{\text{ev}} = 3000$ and $N_{\text{toy}} = 50000$. This number will be used throughout this report as it is a reasonable approximation of the expected number of events on the 2011+2012 data sample.

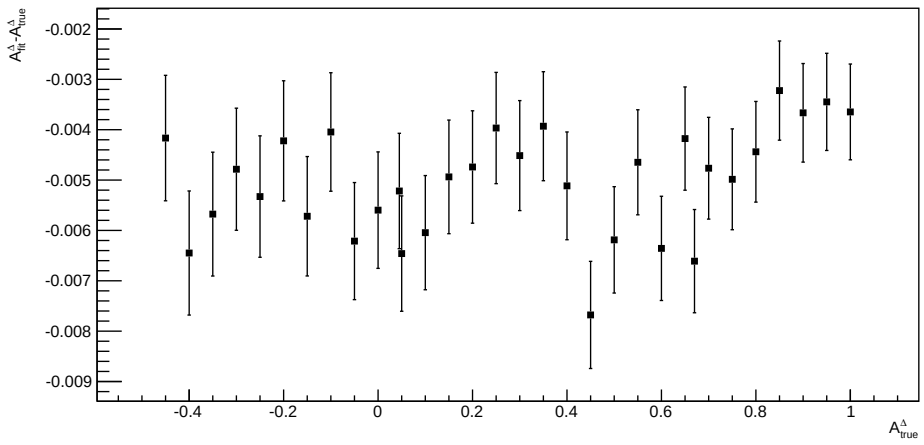

Figure 10: Bias for pure toys depending on the true value of $\mathcal{A}^\Delta$, with 3000 events and 50 000 toys

Figure 10 shows this dependency. The bias is constant (the slope is 0.0009 ± 0.0006) and has a value of -0.0053 ± 0.0003 which is 10% of the value value expected in the SM, $\mathcal{A}^\Delta = 0.045$.

5 Acceptance

The p.d.f. described by Eq. 8 is the generated time-dependent decay rate but does not take into account effect of the detector and event selection, which generates a non-constant efficiency as a function of proper time. Detection of B mesons depends on the proper time and justifies an acceptance function also depending on the proper time. This acceptance function is described by:

$$\epsilon(t) = \epsilon_{\text{low}}(t) \times \epsilon_{\text{high}}(t), \tag{17}$$

where

- ϵ_{low} represents the part affecting low proper times

$$\epsilon_{\text{low}}(t; t_0, a, n) = \frac{a(t-t_0)^n}{1 + a(t-t_0)^n}$$

- ϵ_{high} affect the high proper times

$$\epsilon_{\text{high}}(t; \beta) = (1 - \beta t)$$

This then gives for the full acceptance:

$$\epsilon(t) = \frac{a(t-t_0)^n}{1 + a(t-t_0)^n} (1 - \beta t) \tag{18}$$

Therefore the full considered p.d.f. will be given by:

$$(\epsilon \times \Gamma_{B_s})(t) = \frac{a(t-t_0)^n}{1 + a(t-t_0)^n} (1 - \beta t) \left(e^{-\Gamma_s t} \left(\cosh(\frac{\Delta\Gamma_s t}{2}) - \mathcal{A}^{\Delta} \sinh(\frac{\Delta\Gamma_s t}{2}) \right) \right) \tag{19}$$

The parameters a, n, t_0 and β are given externally in our case and the used values can be found in Table 3. The methods used for extracting the parameters are beyond the scope of this project.

Parameters	$B_S^0 \to \phi\gamma$
a	(3.0 ± 0.3) ps^{-1}
n	(1.8 ± 0.1)
t_0	(0.19 ± 0.01) ps^{-1}
β	(32 ± 6) fs^{-1}

Table 3: Experimental parameters used for the acceptance, taken from [6]

Figure 11 show the acceptance function described in Eq. 18 and Fig. 12 show the time-dependent decay rate with the acceptance taken into account. One can see that the acceptance mainly influences the events with low lifetime.

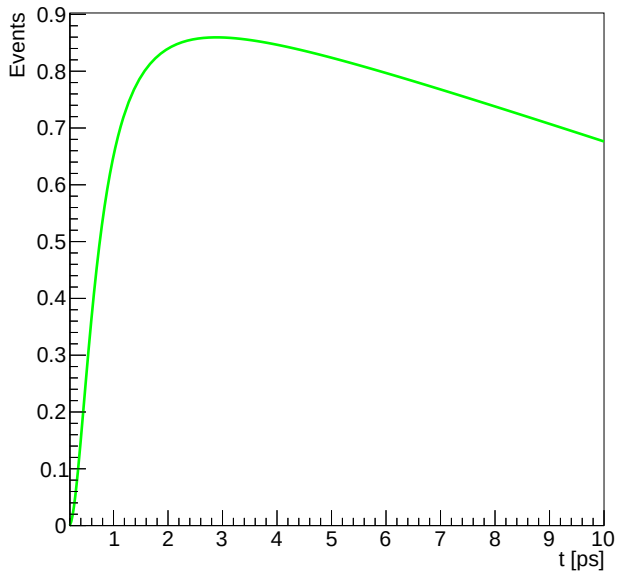

Figure 11: Acceptance function

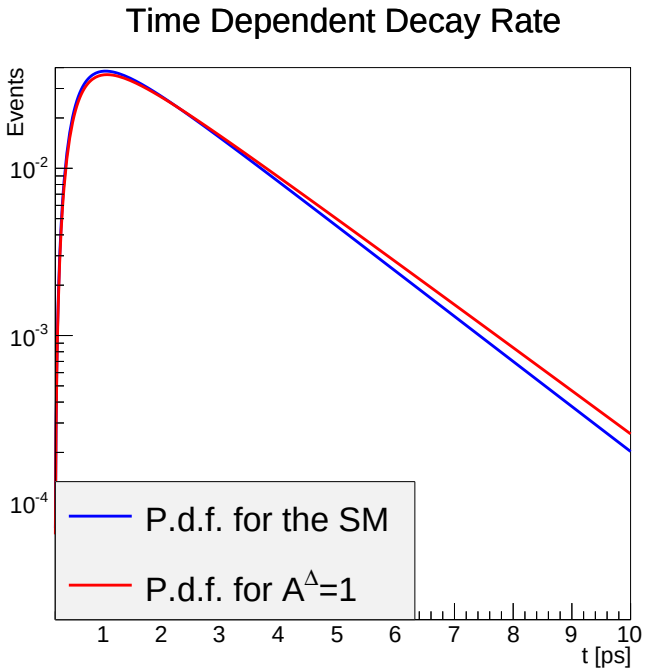

Figure 12: Time-dependent decay rate for $B_S^0 \to \phi\gamma$ taken the acceptance into acount

6 Method for Monte Carlo toys with experimental effects

To study parameter $\mathcal{A}^\Delta$ we generate Monte Carlo toys according to the p.d.f. from Eq. 19. For each of these toys we retrieve the value of $\mathcal{A}^\Delta$ and of the pull of $\mathcal{A}^\Delta$ as explained in section 4. The idea is then to implement step by step the different effects that will dilute the sensitivity of $\mathcal{A}^\Delta$, such as:

- The uncertainty on the acceptance parameters
- The uncertainty on the B_s meson parameters τ_s and $\Delta\Gamma_s$
- The proper time resolution

The generation of the toys is done using `RooMCStudy` . Each set of MC simulation contains $N_{\text{ev}} = 3000$ events and $N_{\text{toy}} = 50000$ toys. As explained in section 4.2 N_{ev} is chosen as to represent the number of events to be expected in the 2011+2012 data sample. For now we focus on the SM and all toys are generated with $\mathcal{A}^\Delta = 0.045$.

In order to asses the sensitivity of $\mathcal{A}^\Delta$, we will use confidence belts created using the Neyman construction [1] which scans $\mathcal{A}^\Delta$. For each value of $\mathcal{A}^\Delta$ we want to find the confidence interval for 1, 2 or 3 standard deviations. The observed variable $\mathcal{A}^\Delta_{\text{obs}}$ is distributed according to a function $f(\mathcal{A}^\Delta_{\text{obs}}|\mathcal{A}^\Delta)$ and we want to find $\mathcal{A}^\Delta_{\text{low}}$ and $\mathcal{A}^\Delta_{\text{up}}$ such that

$$\mathcal{A}^\Delta_{\text{low}} \leq \mathcal{A}^\Delta \leq \mathcal{A}^\Delta_{\text{up}}, \tag{20}$$

contains the true value $\mathcal{A}^\Delta_0$ with probability α, α is either $1\sigma = 68.27\%$, $2\sigma = 95.45\%$ or $3\sigma = 99.73\%$.
This can be rewritten as :

$$\alpha = \int_{\mathcal{A}^\Delta_{\text{low}}}^{\mathcal{A}^\Delta_{\text{up}}} f(\mathcal{A}^\Delta_{\text{obs}}|\mathcal{A}^\Delta) d\mathcal{A}^\Delta \tag{21}$$

In order to obtain a confidence belt we need to "invert" the Eq. 21 using a Neyman construction [1]. We are looking for an interval in $\mathcal{A}^\Delta_{\text{obs}}$ space: $[\mathcal{A}^\Delta_{\text{low}}(\mathcal{A}^\Delta), \mathcal{A}^\Delta_{\text{up}}(\mathcal{A}^\Delta)]$, but this solution is not unique, because an ordering algorithm is necessary to choose how events get included in the interval. We choose to use the central interval criterion, that is we fix:

$$\int_{-\infty}^{\mathcal{A}^\Delta_{\text{low}}} f(\mathcal{A}^\Delta_{\text{obs}}|\mathcal{A}^\Delta) d\mathcal{A}^\Delta = \frac{1-\alpha}{2} = \int_{\mathcal{A}^\Delta_{\text{up}}}^{\infty} f(\mathcal{A}^\Delta_{\text{obs}}|\mathcal{A}^\Delta) d\mathcal{A}^\Delta \tag{22}$$

Figure 13 is an example of the application of this method, where we can see the confidence interval up to 4 σ.

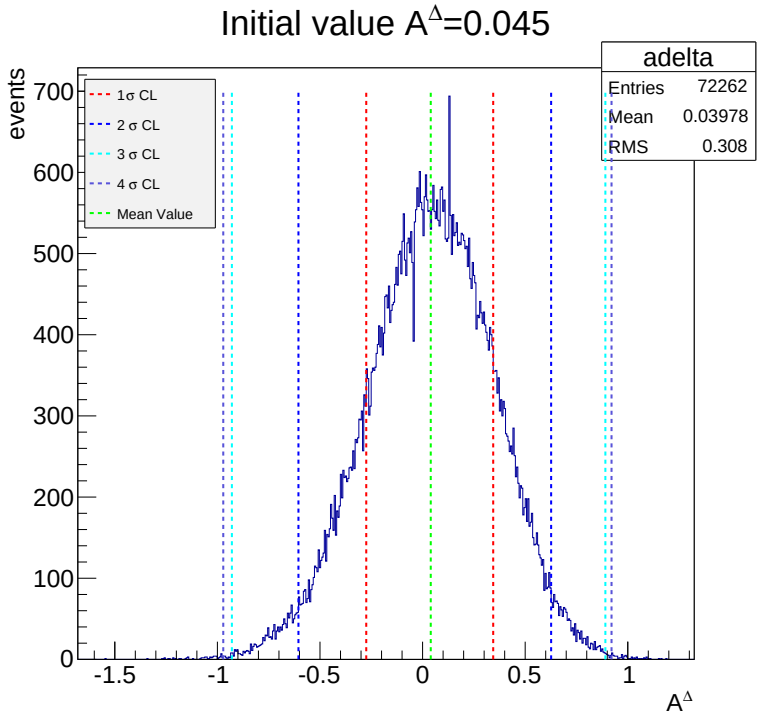

Figure 13: Distribution of $\mathcal{A}^{\Delta}$ for an initial value of 0.045, confidence intervals for 1σ, 2σ, 3σ and 4σ

Other possible choice would have been the upper limit, the lower limit, or the Feldman-Cousins ordering principle [2], [3].

Monte Carlo Neyman construction are realized by scanning the parameter of interest, in our case $\mathcal{A}^{\Delta}$. For each value of true $\mathcal{A}^{\Delta}$ we retrieve the lower and upper limit ($\mathcal{A}^{\Delta}_{\text{low}}$ and $\mathcal{A}^{\Delta}_{\text{up}}$) and then plot this as a function of $\mathcal{A}^{\Delta}$ to visualize the belt. The belt is constructed vertically and allows us to determine the confidence interval on the observed data, horizontally.

We can use the Neyman construction to add the different effect listed earlier to $\mathcal{A}^{\Delta}$ and see how the confidence belts evolve. We generate 2 types of toys to which we then add effects such as resolution or parameter uncertainty:

- Toys with acceptance using the Eq. 18
- Toys with acceptance using $\beta = 0$ in Eq. 18

Figure 14 represents the confidence belts obtained with this method for pure toys with no effect. One can see that already for the simplest case, for an observed value of $\mathcal{A}^{\Delta} = 0.045$ with a probability of 3σ, the range of possible true values for $\mathcal{A}^{\Delta}$ covers the full physically allowed range.

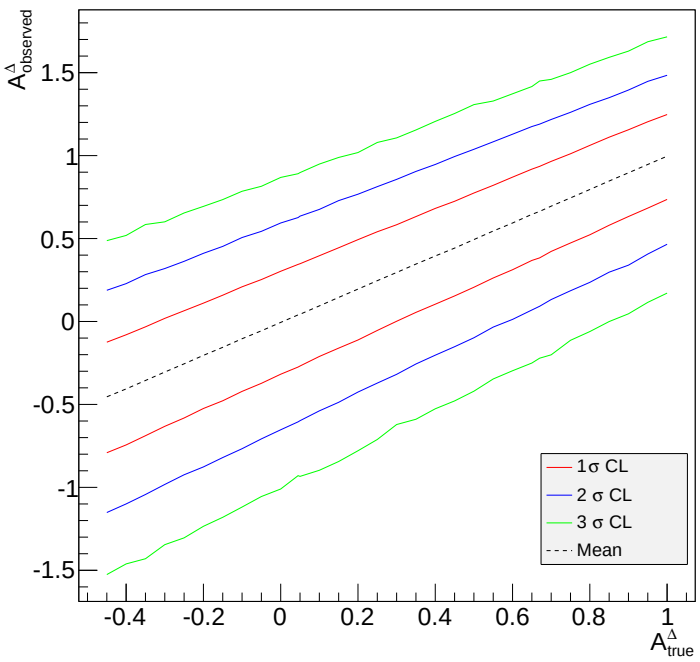

Figure 14: Confidence Belts for pure toys with no effects, 1σ, 2σ and 3σ

Confidence belts are then used to compute the added uncertainties by the different effects. For this we will use 1σ belt. The procedure is the following:

- Compute the confidence belt for two different toys labeled 1 and 2
  - Confidence belt 1 does not have the studied effect
  - Confidence belt 2 incorporates the studied effect
- For a true value $\mathcal{A}^{\Delta}_{\text{true}} = 0.045$ recover the expected observed mean $\mathcal{A}^{\Delta}_{\text{obs, mean}}$. This is chosen in order to give the results but can be repeated for all other $\mathcal{A}^{\Delta}_{\text{true}}$ with the help of the belt.
- Find the width of the two belt at this mean value, meaning $\mathcal{A}^{\Delta}_{\text{low}}(\mathcal{A}^{\Delta}_{\text{obs,mean}})$ and $\mathcal{A}^{\Delta}_{\text{up}}(\mathcal{A}^{\Delta}_{\text{obs,mean}})$ for each confidence belt
- Compute the uncertainty in $\mathcal{A}^{\Delta}$ as in equation: $\sigma = \frac{1}{2}\left(\mathcal{A}^{\Delta}_{\text{up}}(\mathcal{A}^{\Delta}_{\text{obs,mean}}) - \mathcal{A}^{\Delta}_{\text{low}}(\mathcal{A}^{\Delta}_{\text{obs,mean}})\right)$, for each belt
- Compute the added uncertainty using the difference in the quadrative:

$$\sigma_{\text{add}} = \sqrt{\sigma_2^2 - \sigma_1^2}, \tag{23}$$

  where
  - σ_{add} is the added uncertainty due to the effect
  - σ_1 is the uncertainty for the toys without the studied effect
  - σ_2 is the uncertainty of the toys with the studied effect

This method is used to quantify the different experimental effect such as the acceptance, the resolution or the uncertainty of certain parameters. In addition the means of the $\mathcal{A}^{\Delta}$ distributions will be used to quantify the bias induced by each effect.

7 Toys with acceptance

Let us start by adding the acceptance as described in Eq. 18 to the toys. On Fig. 15 we can see the distribution of $\mathcal{A}^{\Delta}$ and of its pull for $N_{\text{toy}} = 50000$ toys of $N_{\text{ev}} = 3000$ events each. If we compare this to figure 6 we can see that the mean value of $\mathcal{A}^{\Delta}$ is slightly higher, that is, a larger statistical bias is induced by the presence of the acceptance.

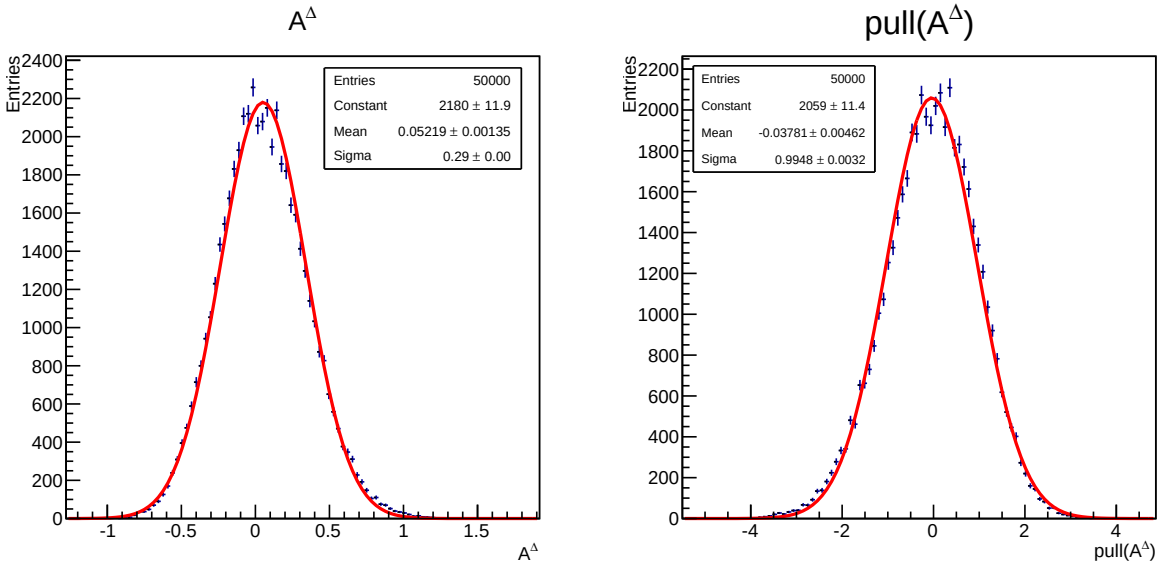

Figure 15: Distribution of $\mathcal{A}^\Delta$ and pull($\mathcal{A}^\Delta$) with acceptance for $N_{\text{ev}} = 3000$ and $N_{\text{toy}} = 50000$

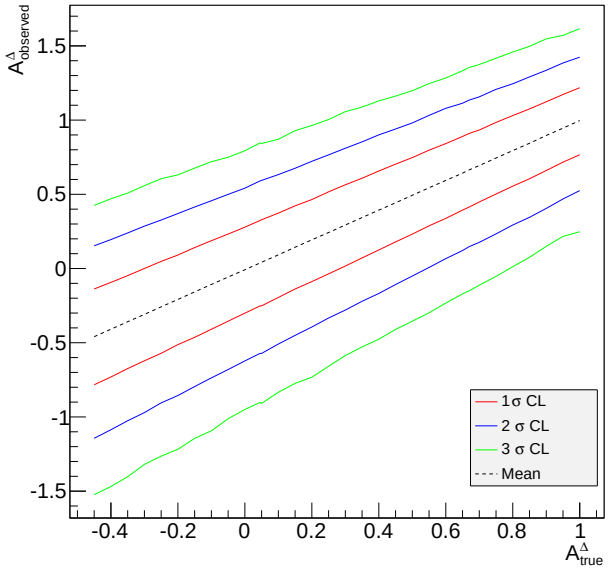

Figure 16: Confidence belts for toys with acceptance for 1σ, 2σ and 3σ.

7.1 Uncertainty on acceptance parameters

As can be seen in Eq. 18, the expression for the acceptance depends on 4 parameters. Since they are fixed in the fit, uncertainties on these parameters would induce imprecision on the measurement of $\mathcal{A}^{\Delta}$. If these values are fixed in the fit, we thus need to take into account the fact that we might be wrong about these value. In order to do this we generate toys with the current values of either a, n, t_0 or β that we consider to be the "right" value and fit with a "wrong" to simulate our ignorance. Initially this is done separately for each parameter, and afterwards we will combine the uncertainties. While one parameter is being studied and scanned, the other ones remains fixed. The "right" or fixed values of the parameters are taken from Table 3.
Then, each parameter is scanned in the following ranges:

- $a \in [a - 5\sigma, a + 5\sigma] = [1.50, 4.50]$ ps^{-1},
- $n \in [n - 5\sigma, n + 5\sigma] = [1.30, 2.30]$,
- $t_0 \in [t_0 - 5\sigma, t_0 + 5\sigma] = [0.14, 0.24]$ ps^{-1}
- $\beta \in [\beta - 5\sigma, \beta + 5\sigma] = [0.002, 0.062]$ ps^{-1}

The 5σ choice is done for statistical reasons. It allows us to cover 99.99994% of the possible range of the parameter and to better understand the trends. Figures 17, 18, 19, 20 show the influence of the different parameters present in the acceptance on the precision of $\mathcal{A}^{\Delta}$. Clearly all the parameters strongly influence the measurement of $\mathcal{A}^{\Delta}$ both in terms of bias and sensitivity, and will have to be known precisely.
Let us notice that the scan of offset parameter t_0 yields a surprising none linear response. It appears as if for small values of t_0 the measurement of mean of $\mathcal{A}^{\Delta}$ is strongly affected whereas the width of the distribution of $\mathcal{A}^{\Delta}$ is stable.

7.2 Confidence belts

We use the method described in section 6 to determine the added uncertainty by the acceptance.

In order to properly study the overall effect of the uncertainty in the acceptance parameters, we also need to take their correlations into account. To do so, toys are performed by generating data fluctuating the values of these parameters according to a multivariate Gaussian with the suitable covariance matrix and fitting them with the acceptance parameters fixed to their nominal values.

Figure 21 shows the confidence belt for toys with acceptance and fixed parameters and for toys with acceptance and uncertainties on all acceptance

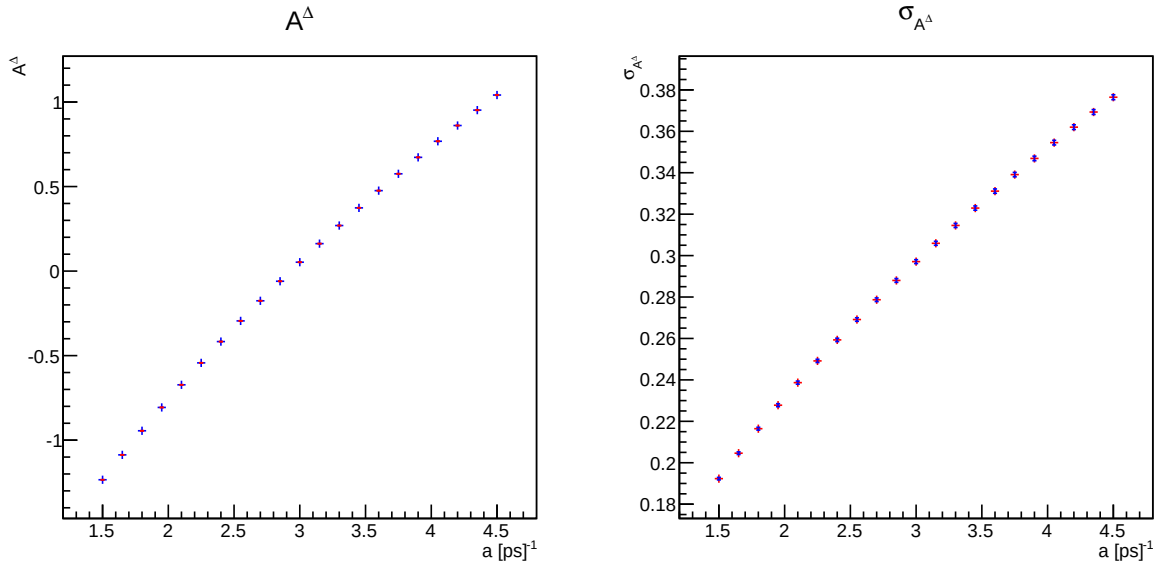

Figure 17: Fitted value of $\mathcal{A}^\Delta$ using varying fit value of a acceptance parameter, for initial $\mathcal{A}^\Delta = 0.045$, 3000 events and 50000 toys

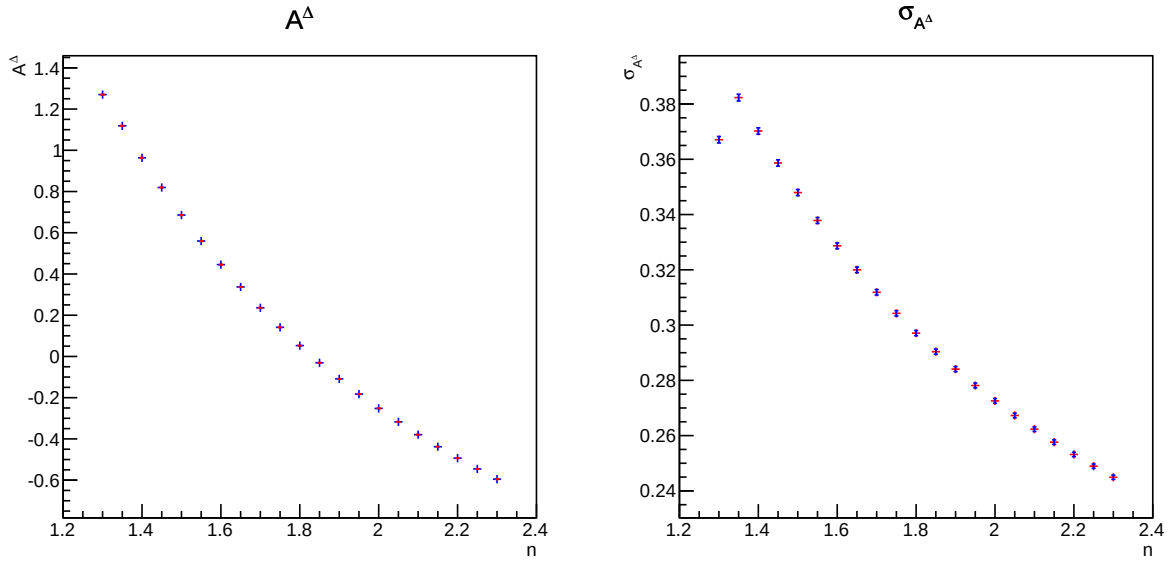

Figure 18: Fitted value of $\mathcal{A}^\Delta$ using varying fit value of n acceptance parameter, for initial $\mathcal{A}^\Delta = 0.045$, 3000 events and 50000 toys

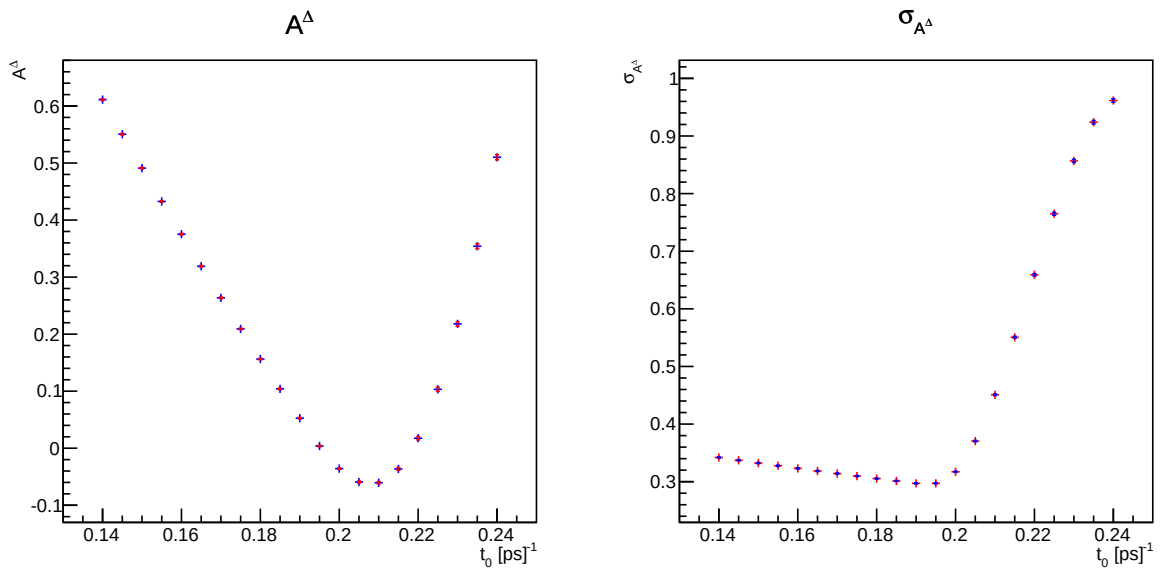

Figure 19: Fitted value of $\mathcal{A}^{\Delta}$ using varying fit value of t_0 acceptance parameter, for initial $\mathcal{A}^{\Delta} = 0.045$, 3000 events and 50000 toys

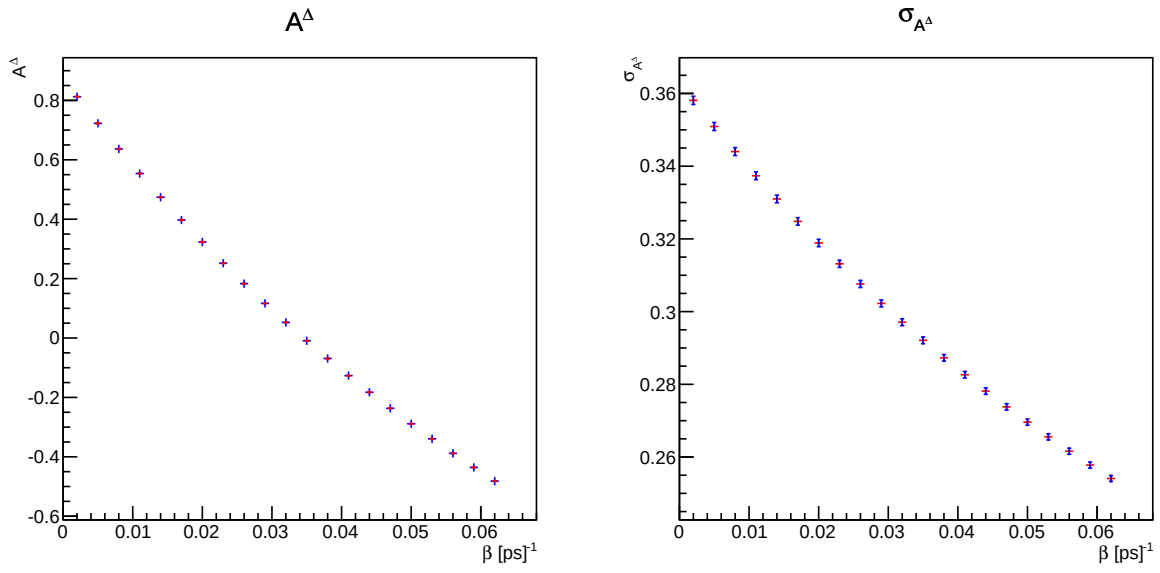

Figure 20: Fitted value of $\mathcal{A}^{\Delta}$ using varying fit value of β acceptance parameter, for initial $\mathcal{A}^{\Delta} = 0.045$, 3000 events and 50000 toys

parameters. We can use this to quantify the added uncertainty, comparing the toys with the studied effect with toys without it, and find $\sigma_{\text{add, acc, float}} = 0.4243$. The mean values as well as the upper and lower limits are in Table 4

Parameters	**Acceptance**	**Uncertainty acceptance parameters**
Mean value	0.0370354	-0.0119727
Lower limit	-0.2615	-0.5373
Upper limit	0.3187	0.4906

Table 4: Confidence intervals for toy with acceptance and acceptance with uncertainty on all acceptance parameters, N_{ev} =3000, N_{toy} = 50000 at $\mathcal{A}^{\Delta}_{\text{true}}$=0.045

This effect is very important compared to the statistical error and as we will see in the next section compared to the uncertainty due to imprecisions on the input parameters τ_s and $\Delta\Gamma_s$ and . In order to refine the measurement of $\mathcal{A}^{\Delta}$ we need a higher precision on the acceptance parameters.

Figures 22 shows the same two band as Fig. 21 and in addition the confidence belt of toys with acceptance but $\beta = 0$ meaning that only ϵ_{low} contributes. Let us notice that the belt with $\beta = 0$ is slightly wider than the ones with the full acceptance. This would mean that adding the shape due to ϵ_{high} makes it easier to fit $\mathcal{A}^{\Delta}$.This contribution acts mainly on the tail of the p.d.f. described by Eq. 8 which is the most sensitive to $\mathcal{A}^{\Delta}$. It is also worth noting that even though the acceptance doesn't deteriorate the sensitivity of the measurement of $\mathcal{A}^{\Delta}$, the uncertainties of its parameters will.

8 Uncertainty on B_s mesons parameters

Equation 8 contains the B_s lifetime $\tau_s = 1/\Gamma_s$ and the width difference $\Delta\Gamma_s$. Uncertainties on these parameters could affect the measurement of $\mathcal{A}^{\Delta}$, and should be investigated. Just as for the acceptance parameters, we generate toys with the "right" value of the parameter and then fit with a "wrong" fixed value. The "right" values as well as the fixed parameter are taken from in Table 1.
We scan the parameter in the following ranges:

- $\tau_s \in [\tau_s - 5\sigma, \tau_s + 5\sigma] = [1.461, 1.571]$ ps , and $\Delta\Gamma_s = 0.081\text{ps}^{-1}$

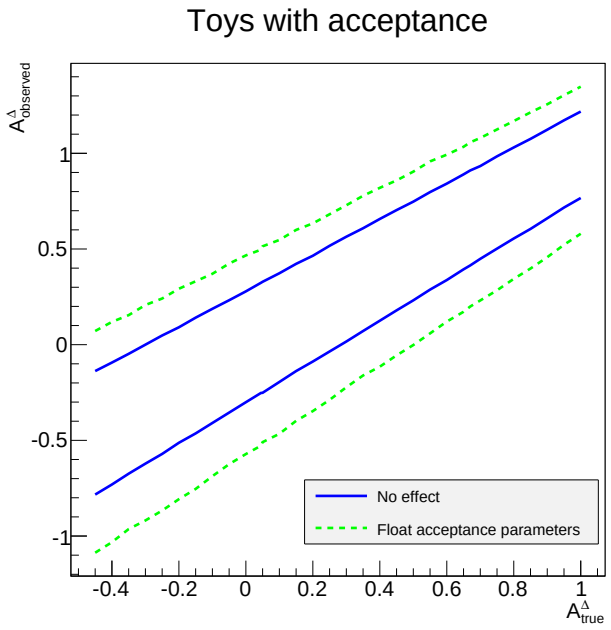

Figure 21: Confidence belts for toys with acceptance and fixed parameters, and toys with acceptance and uncertainties on acceptance parameters, both for 1σ

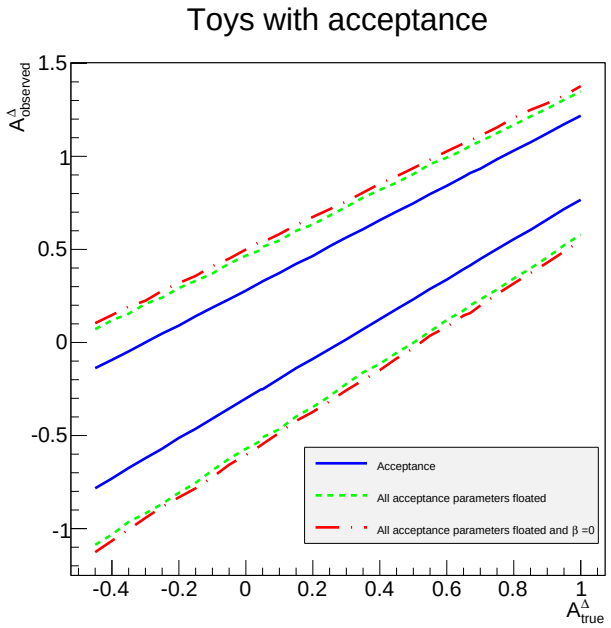

Figure 22: Confidence belts for toys with acceptance, first with no effect, then with uncertainties on acceptance parameters and finally with uncertainties on acceptance parameters and $\beta = 0$, all for 1σ confidence level

– $\Delta\Gamma_s \in [\Delta\Gamma_s - 5\sigma, \Delta\Gamma_s + 5\sigma] = [0.026, 0.136]\text{ps}^{-1}$, and $\tau_s = 1.516$ ps.

8.1 Lifetime τ_s

On Fig. 23 one can see the effect of varying τ_s, $\Delta\Gamma_s$ is fixed and there is not acceptance or resolution. The effect on $\mathcal{A}^\Delta$ of an uncertainty on τ_s is important and thus can not be neglected.

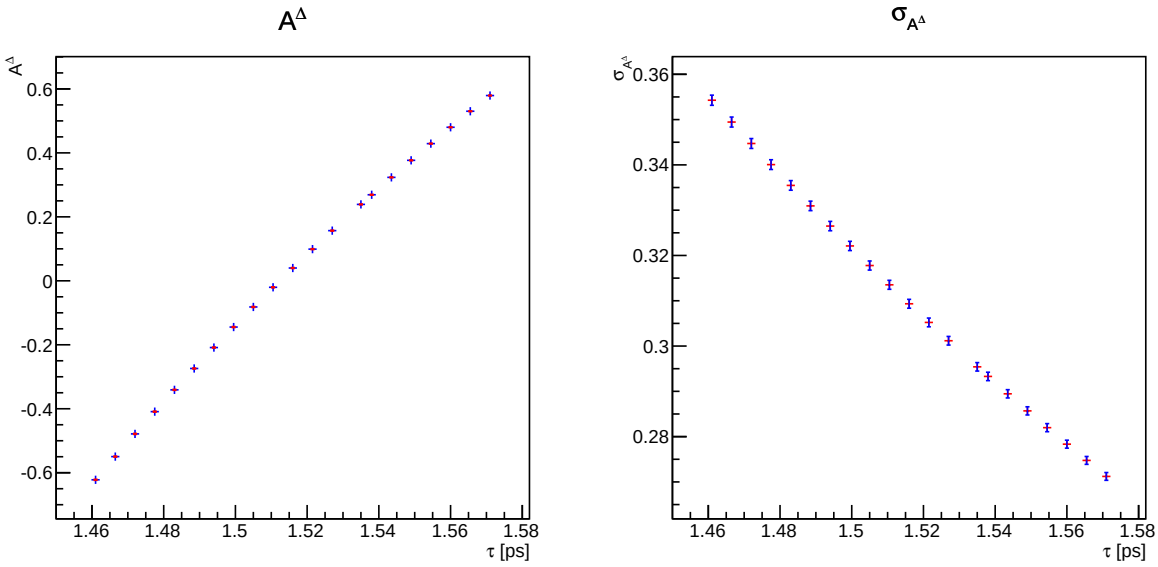

Figure 23: Fitted value of $\mathcal{A}^\Delta$ using varying fit value of τ_s for initial $\mathcal{A}^\Delta = 0.045$, N_{ev} =3000 events and N_{toy} =50 000 toys

Let us notice that for high values of τ_{fit} the fitted value of $\mathcal{A}^\Delta_{\text{fit}}$ is far from the input value of $\mathcal{A}^\Delta$ =0.045, but $\sigma_{\mathcal{A}^\Delta}$ diminishes.Therefore large values of τ_s cause a large bias in $\mathcal{A}^\Delta$ as it tries to compensate the change in the exponential but at the same time the sensitivity improves because the dominance of the exponential term diminishes. Let us look at the distribution of $\mathcal{A}^\Delta$ is this case and at the pull($\mathcal{A}^\Delta$) on Fig. 24. One can notice that the pull($\mathcal{A}^\Delta$) indicates a totally biased fit as the mean value is far from 0. In addition the error is not correct as the width of the pulls gaussian is not 1, showing that we are far from the asymptotic regime.

In order to quantify the uncertainty added by an imprecise knowledge of the parameters, we use the confidence belts as explained in section 6. The belts are generated by fitting applying a Gaussian constraint on τ_s (as is hope to be done on data) with mean and width given by the values in Table 1.
Figure 25 shows the confidence belts for toys with acceptance and fixed τ_s

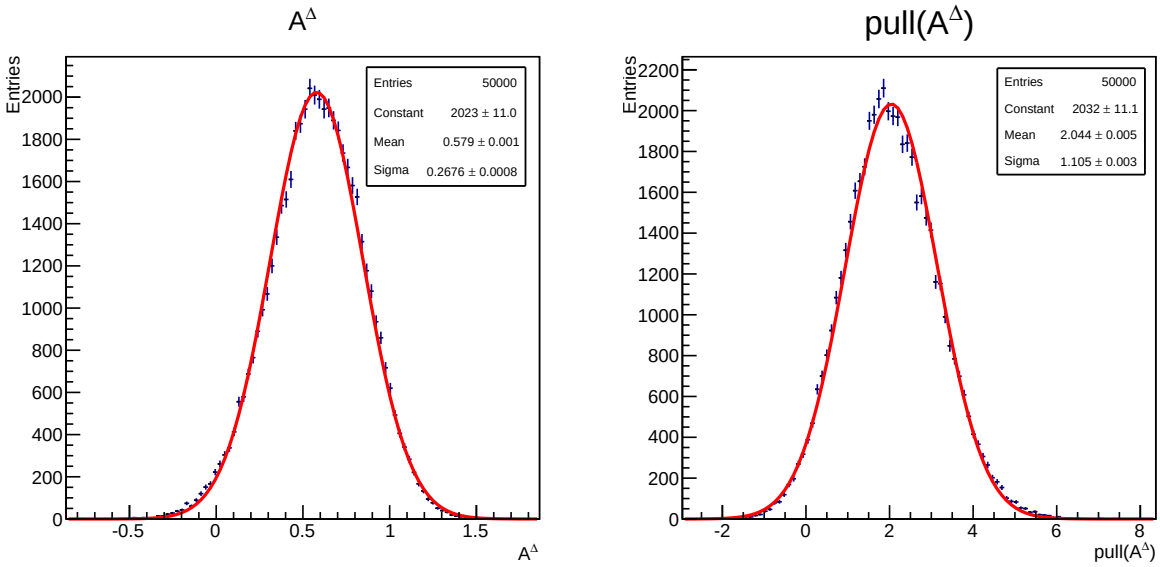

Figure 24: Distribution of $\mathcal{A}^\Delta$ and pull($\mathcal{A}^\Delta$) for an initial value of $\tau_{\text{ini}} = 1.516$ and a fitted value of $\tau_{\text{fit}} = 1.571$ for $N_{\text{ev}} = 3000$ and $N_{\text{toy}} = 50000$

and for the toys with acceptance and τ_s fitted applying a Gaussian constraint.

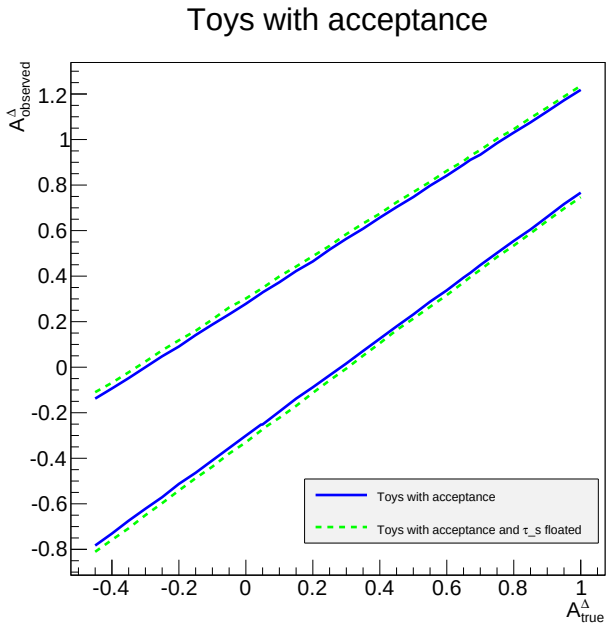

Figure 25: Confidence belts for toys with acceptance and no effects, and for toys with acceptance and a Gaussian constraint on τ_s both for 1σ

The mean observed value for an input of $\mathcal{A}^{\Delta}_{\text{true}} = 0.045$, as well as the interval of true values corresponding to this observed mean, for both the toys with acceptance and with a Gaussian constraint on τ_s are shown in Table 5. The values for the toy with acceptance but no effect are in Table 4

Parameters	Mean Value	Lower Limit	Upper Limit
Gaussian constraint on τ_s	0.0372	-0.2874	0.3381

Table 5: Confidence intervals for toys with acceptance and uncertainties on τ_s, N_{ev} =3000, N_{toy} = 50000 at $\mathcal{A}^{\Delta}_{\text{true}}$=0.045

We can then use Eq. 23 to compute the effect of the Gaussian constraint on τ_s, on $\mathcal{A}^{\Delta}$, and find $\sigma_{\text{add},\tau_s} = 0.1169$.

8.2 Width difference $\Delta\Gamma_s$

Figure 26 represents the effect of $\Delta\Gamma_s$ on $\mathcal{A}^{\Delta}$. Let us notice that the dependance of $\mathcal{A}^{\Delta}$ on $\Delta\Gamma_s$ is not linear and more important for smaller values of $\Delta\Gamma_s$. This is reflected in the mean value of $\mathcal{A}^{\Delta}$ as well as in the sensitivity $\sigma_{\mathcal{A}^{\Delta}}$, hence for small values of $\Delta\Gamma_s$ we retrieve a strongly biased value with a large uncertainty. As a result the pull of the distribution of $\mathcal{A}^{\Delta}$ is strongly biased as can be seen on Fig. 27. However close to the PDG value $\Delta\Gamma_s = 0.081$ the effect both on the mean and on the sensitivity is decreased. This results in a small induced sensitivity, and a small additional bias on $\mathcal{A}^{\Delta}$.

Let us use the confidence belts to quantify the induced uncertainty of $\Delta\Gamma_s$ on $\mathcal{A}^{\Delta}$. As for τ_S the toys are generated applying a Gaussian constraint on $\Delta\Gamma$ with mean and width corresponding to the value given in Table 1, using toys with acceptance.

Results are on Fig. 28 and as expected, as the mean value of $\Delta\Gamma$ is high, the addition of a Gaussian constraint on $\Delta\Gamma_s$ barely affect the confidence belt.
Table 6 contains the mean observed value for a true value of $\mathcal{A}^{\Delta}_{\text{true}} = 0.045$ as well as the 1 σ confidence interval of this mean.
Using Eq. 23 it allows us to compute the induced uncertainty when $\Delta\Gamma_s$ is constraint and we find $\sigma_{\text{add},\Delta\Gamma_s}$=0.0465. This value, as expected, is smaller than that obtained for τ_s and could easily be neglected.

8.3 Gaussian constraint on both τ_s, $\Delta\Gamma_s$

This last configuration is the one expected to be used in the fit to the data. Figure 29 shows the confidence belts for 1σ, for toy with acceptance

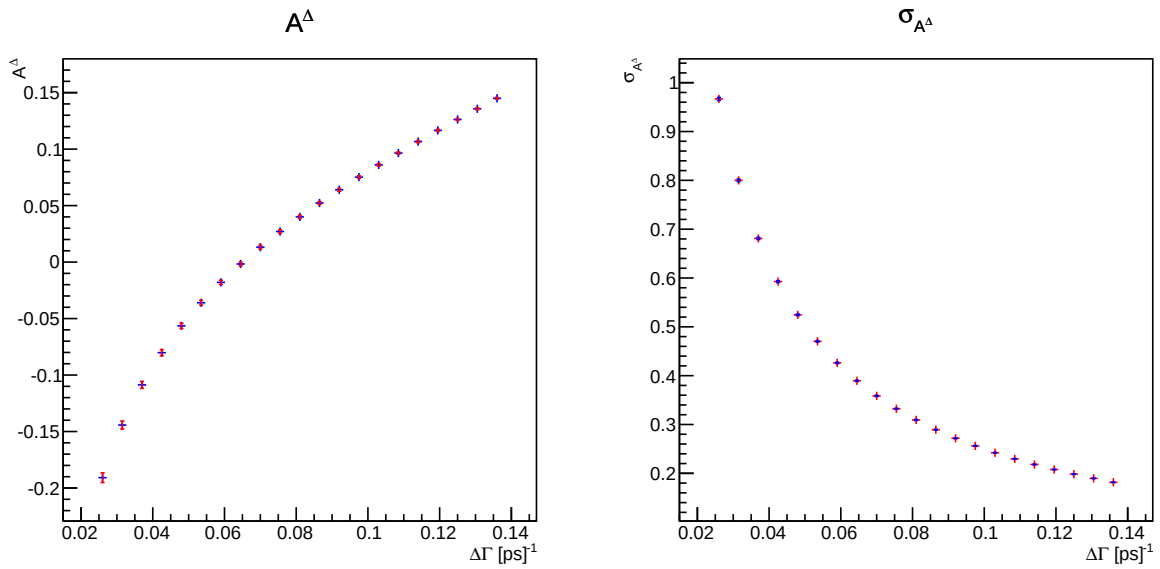

Figure 26: Fitted value of $\mathcal{A}^\Delta$ using varying fit value of $\Delta\Gamma_s$ for initial $\mathcal{A}^\Delta$ = 0.045, N_{ev} = 3000 events and N_{toy} =50000 toys

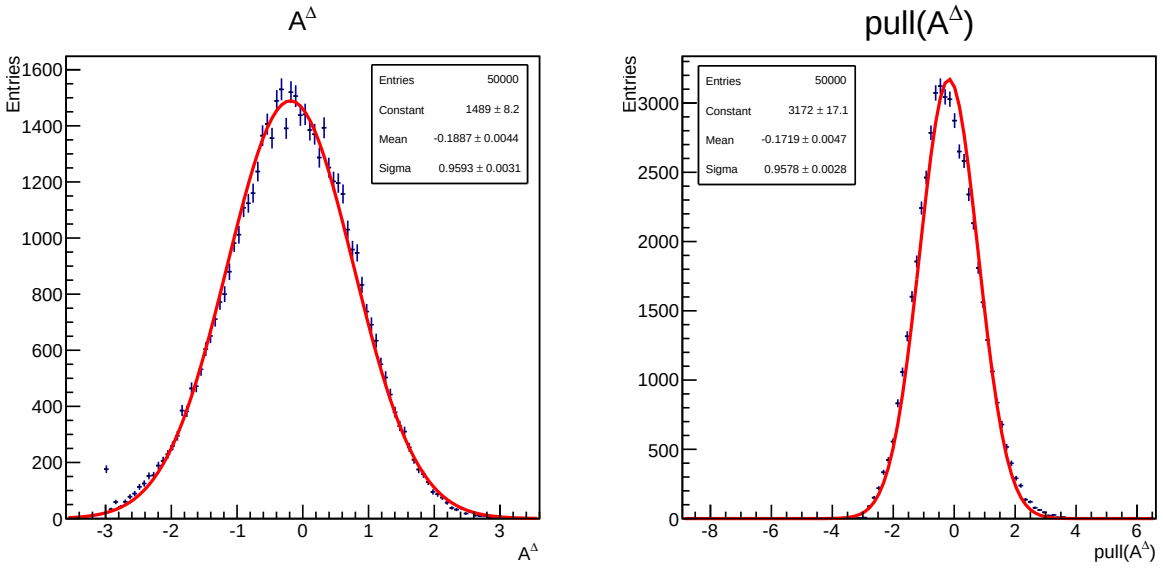

Figure 27: Distribution of $\mathcal{A}^\Delta$ and pull($\mathcal{A}^\Delta$) for an initial value of $\Delta\Gamma_{s,\text{ini}}$ = 0.081 and a fitted value of $\Delta\Gamma_{s,\text{fit}} = 0.026$ for $N_{\text{ev}} = 3000$ and $N_{\text{toy}} = 50000$

Parameters	Mean value	Lower Limit	Upper Limit
Gaussian constraint on $\Delta\Gamma_s$	0.03636	-0.2678	0.3198

Table 6: Confidence intervals for toy with acceptance and Gaussian constraint on $\Delta\Gamma_s$, at $\mathcal{A}^{\Delta}_{\text{true}}$=0.045

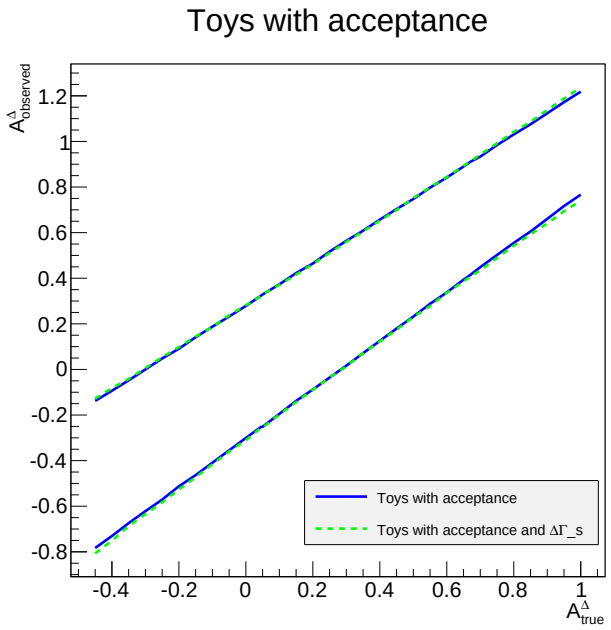

Figure 28: Confidence belts for with acceptance, and for toys with acceptance and with uncertainties on $\Delta\Gamma_s$ both for 1σ

but without any effect, for toys with acceptance and toys with only the lower proper time acceptance and both parameters fitted with a Gaussian constraint. By using the same procedure as before we can compute the added uncertainties by fitting both parameter with a Gaussian constraint. As expected this is the quadratic sum of the uncertainties added by the uncertainty τ_s and those added by fitting $\Delta\Gamma_s$ with a Gaussian constraint. If we compute the added error by fitting both parameters with a Gaussian constraint, using the values in Tables 7 and 5, we obtain $\sigma_{\text{add, both}} = 0.1233$ and if we compute the quadratic sum we find 0.1258.

Figure 30 shows the bias on the mean value of $\mathcal{A}^{\Delta}$ as a function of $\mathcal{A}^{\Delta}$. As expected with each added effect, the bias becomes more important. It is worth noting that the bias decreases with large values of $\mathcal{A}^{\Delta}$. For Gaussian constraint on both B mesons parameters, we get a final bias of $b = 0.0111$ for $\mathcal{A}^{\Delta}$=0.045.

It is worth noting that, should a correlation matrix between these two

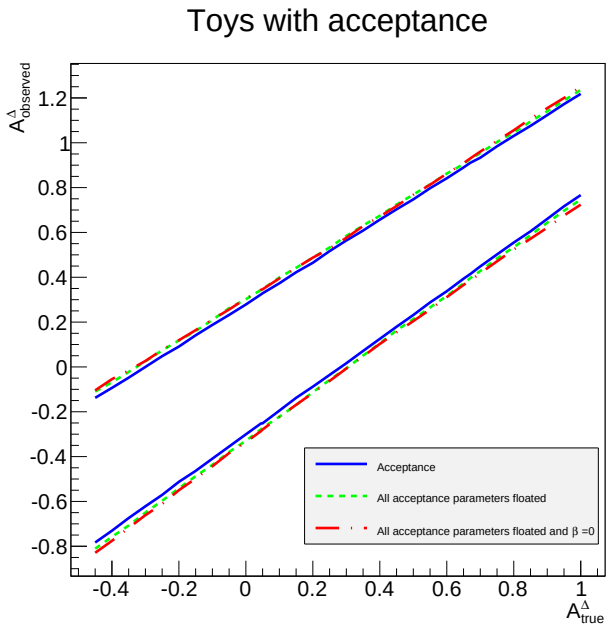

Figure 29: Confidence belts for toys with acceptance and no effects, and for toys with acceptance and uncertainty on τ_s, and for toys with acceptance and both parameters (τ_s and $\Delta\Gamma_s$) fitted with a Gaussian constraint, all for 1σ

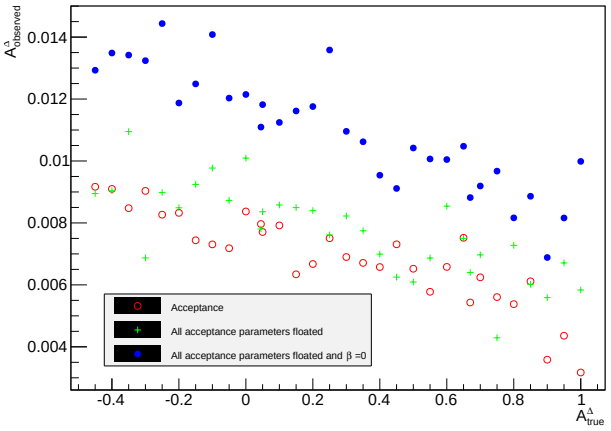

Figure 30: Bias on the mean of $\mathcal{A}^{\Delta}$ for toys with acceptance and no effects, and for toys with acceptance and Gaussian constraint on τ_s, and for toys with acceptance and both parameters (τ_s and $\Delta\Gamma_s$) fitted with a Gaussian constraint, all for 1σ

Parameters	Mean value	Lower Limit	Upper Limit
Gaussian constraint on τ_s and $\Delta\Gamma_s$	0.0339051	-0.2926	0.3378

Table 7: Confidence intervals for toys with acceptance and Gaussian constraint on τ_s and $\Delta\Gamma_s$, at $\mathcal{A}^{\Delta}_{\text{true}}$=0.045

parameters becomes available, this effect would be reduced, as they could be fitted constrained by a 2-dimensional Gaussian.

9 Resolution

The resolution of the detector is generally described by a double gaussian. In order to understand the effect of the resolution, we start by generating events with a resolution represented by a single gaussian of mean μ and width σ. Further on we will go back to the double gaussian resolution.

μ_1	0.00357 ps
σ_1	0.0642 ps
μ_2	0.0157 ps
σ_2	0.1521 ps
f_1	0.622

Table 8: Experimental parameters used for the double gaussian resolution.

As both μ and σ are very small compared to τ_s, we expect that the resolution will have a smaller effect on the measure of $\mathcal{A}^{\Delta}$. To verify this we generate toys with different values of σ, fixing μ, retrieve for each toy $\mathcal{A}^{\Delta}$ and study $\mathcal{A}^{\Delta}$ vs σ. The same is then done to study the effect of μ, by varying the mean of the resolution and fixing σ. The results can be seen on Fig. 39 and 32. As expected the effect of the resolution on the sensitivity of $\mathcal{A}^{\Delta}$ is negligible, however it induces a small bias in the mean value of $\mathcal{A}^{\Delta}$. On figure 32 the mean on $\mathcal{A}^{\Delta}$ is slightly biased by the resolution for small values of the resolution's width but stabilizes around -0.236. This represents large but relatively stable bias.

9.1 Uncertainties on resolution parameters

In addition to this we can study the effect of uncertainties on the resolution parameter. The method is the same as the one employed for the effect of

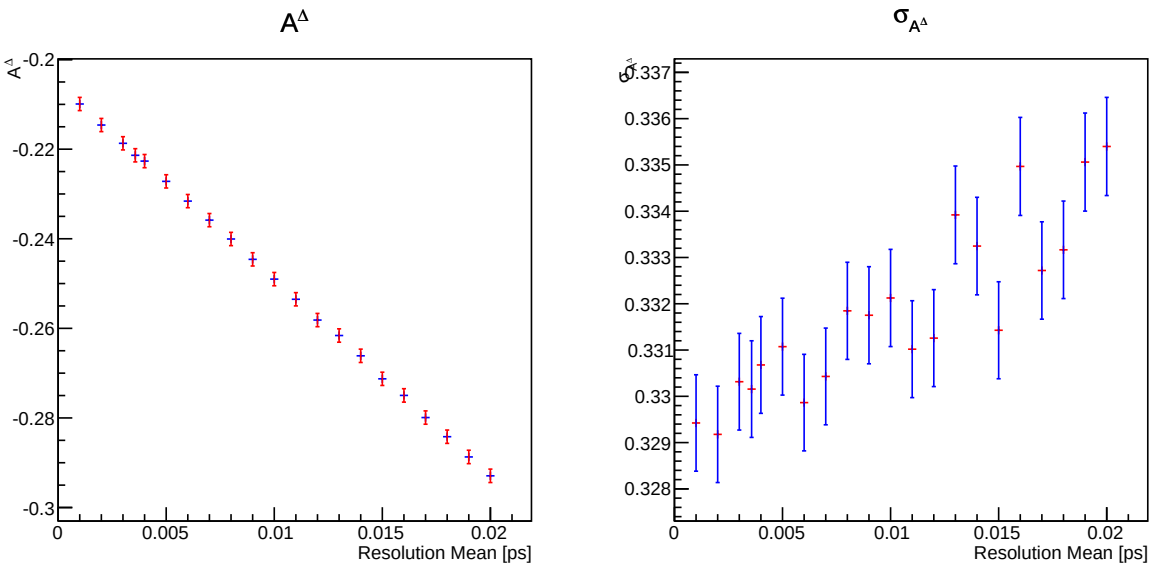

Figure 31: Evolution of $\mathcal{A}^{\Delta}$as a function of the mean of the resolution, N_{ev} = 3000 and N_{toy} = 50000

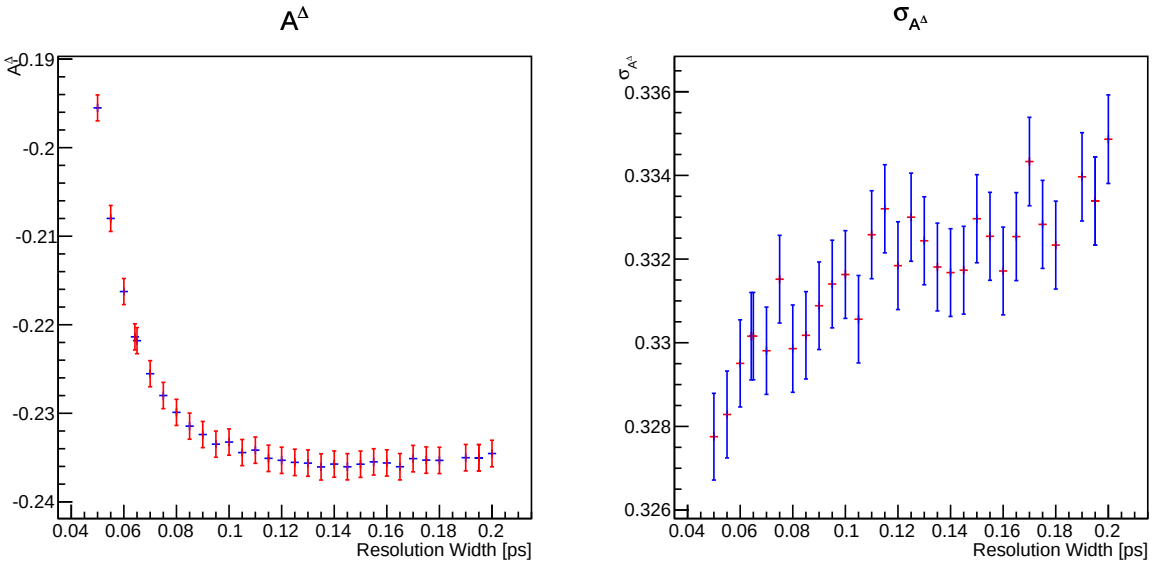

Figure 32: Evolution of $\mathcal{A}^{\Delta}$as a function of the width of the resolution, N_{ev} = 3000 and N_{toy} = 50000

Parameters	Fixed values
Mean μ	3.57 fs
Width σ	64.2 fs

Table 9: Experimental parameters used for the resolution, taken from [6].

the input parameters τ_s and $\Delta\Gamma_s$, and for the acceptance parameters: simulating our ignorance by generating toys with the "right" values and fitted them with "wrong" values.

Imprecision on the resolution parameters would bias the measurement of the mean of $\mathcal{A}^{\Delta}$ as can be seen on figures 33 and 34, but only slightly alter the sensitivity. This means that the value of the resolution is less important as long as it is known precisely.

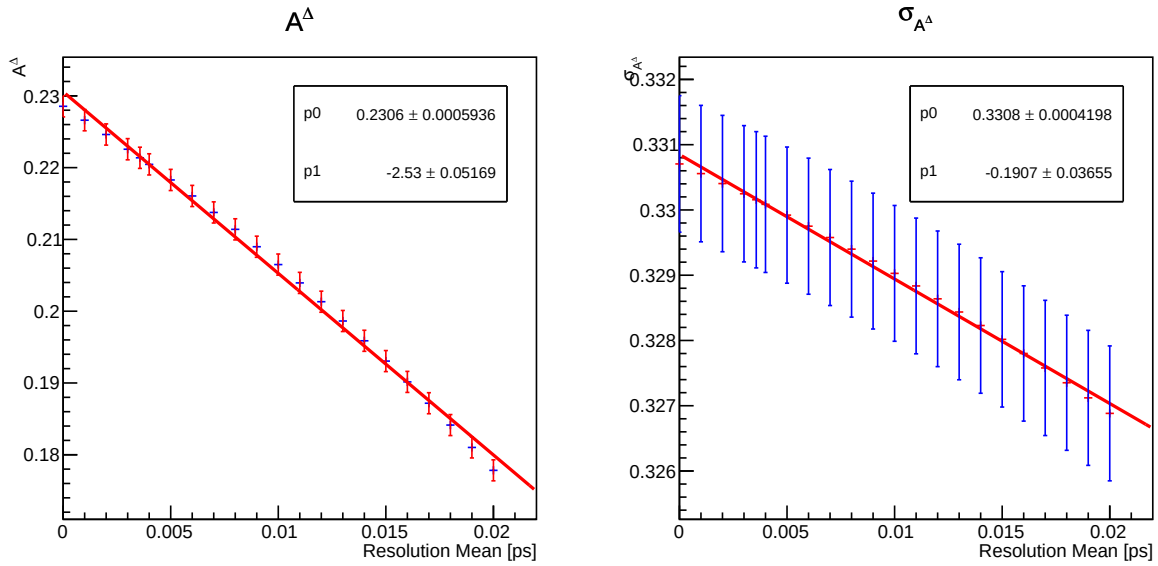

Figure 33: Fitted value of $\mathcal{A}^{\Delta}$ using varying fit values of the mean of the resolution, for initial $\mathcal{A}^{\Delta} = 0.045$, 3000 events and 50 000 toys

As a conclusion the resolution parameters don't affect the sensitivity but cause a large bias in the extraction of $\mathcal{A}^{\Delta}$. Figure 36 represents the bias on the mean value of $\mathcal{A}^{\Delta}$ as a function of $\mathcal{A}^{\Delta}$. As expected adding the resolution, only slightly increases the bias. We can compute the induced bias and find b = 0.0083.

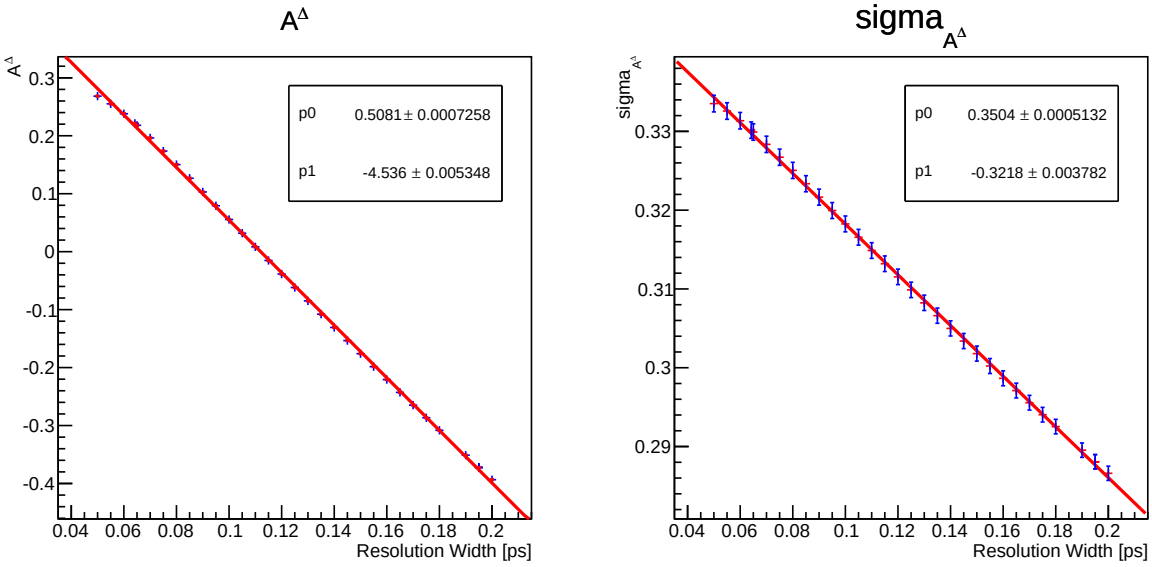

Figure 34: Fitted value of $\mathcal{A}^{\Delta}$ using varying fit values of the width of the resolution for initial $\mathcal{A}^{\Delta} = 0.045$, 3000 events and 50 000 toys

9.2 Confidence belts

As for the previous sections we construct a confidence belt taking into account the effect of the resolution. The results can be see on Fig. 35. As can be expected the resolution has almost no effect on the width on the belt. If we compute the added uncertainty we find $\sigma_{\text{add,res}} = 0.0615$

10 All effects combined

On Fig. 37 we can see the confidence belt including all the studied effects: the acceptance, the uncertainty in its parameters, the resolution and the Gaussian constraint on the B meson properties. For the SM value of $A^{\Delta} = 0.045$, the expected sensitivity is $\sigma_{A^{\Delta}} = 0.4729$. We can also see that, as already observed at the beginning of this study, the sensitivity decreases as the true value of A^{Δ} gets closer to 1, *ie*, the belt gets narrower.

In addition, the total bias is evaluated to be, for $A^{\Delta} = 0.045$, $b = 0.054$. The bias also shows a tendency to decrease as we get to more extreme values, as can be observed by the tilting of the belt with respect to the $A^{\Delta}_{\text{observed}} = A^{\Delta}_{\text{true}}$ line, Fig. 38.

It can also be noted that, with the expected precision, it is not going to be possible to exclude any value of A^{Δ}, since the 3σ belt covers all the possible values of the observable.

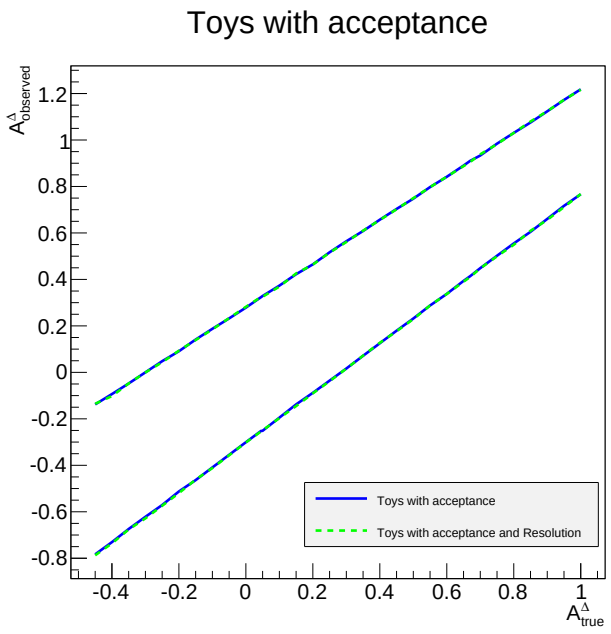

Figure 35: Confidence belts for with acceptance, and for toys with acceptance and resolution both for 1σ

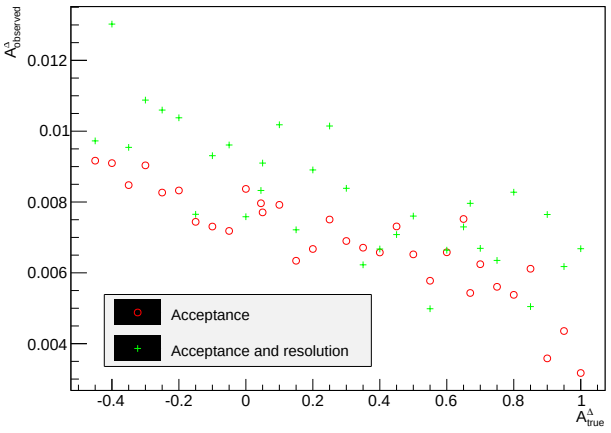

Figure 36: Bias on the mean value of $\mathcal{A}^{\Delta}$ for with acceptance, and for toys with acceptance and resolution both for 1σ

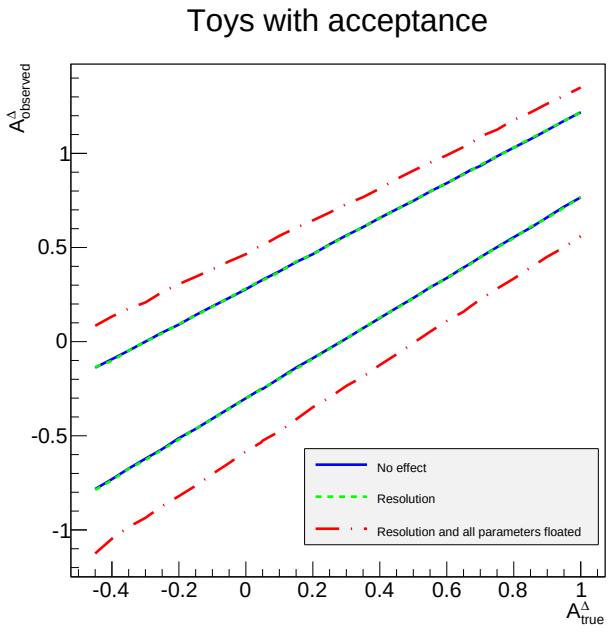

Figure 37: Confidence belts for toys with acceptance, toys with acceptance and resolution, and toys with acceptance, resolution and uncertainties of all parameters, for 1σ.

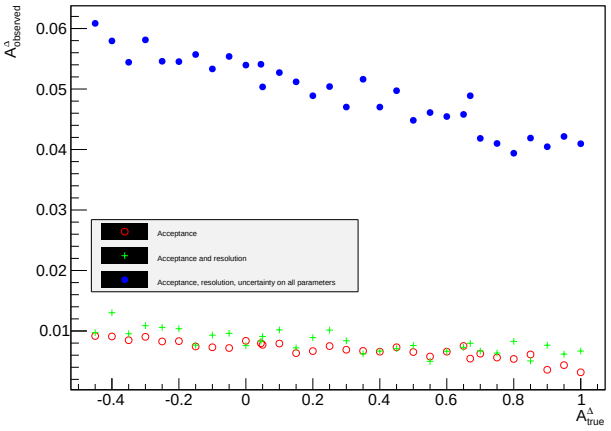

Figure 38: Bias on the mean value of $\mathcal{A}^{\Delta}$ for toys with acceptance, toys with acceptance and resolution and toys with acceptance, resolution and uncertainties of all parameters, for 1σ.

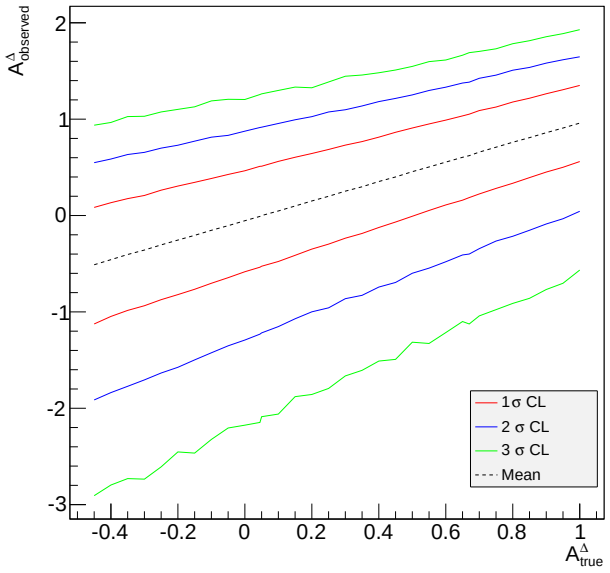

Figure 39: Confidence belts for toys with acceptance, resolution, uncertainties of B mesons parameters and acceptance parameters for 1σ, 2σ and 3σ.

11 Conclusion and future studies

During this study we investigated the different possible experimental effects that can influence the measurement of $\mathcal{A}^{\Delta}$. This allowed us to identify the main sources of errors and imprecisions. A summary of these results can be see in Table 10. Clearly the two main sources of uncertainties are the acceptance parameters and τ_s. Knowing these parameters with higher precision would considerably increase the sensitivity of the measurement of the mean value of $\mathcal{A}^{\Delta}$, and thus increase our chances of distinguishing different possible models.

To these uncertainties we have to add the statistical uncertainty which for $N_{\text{ev}} = 3000$ and $N_{\text{toy}} = 50000$ is 0.2764. This bring us to a total uncertainty of 0.52. The statistical sensitivity will be increased with future data.

Therefore, with the data collected by LHCb in 2011 and 2012, the measurement of A^{Δ} has an expected sensitivty of 0.54. It is worth noting that this measurement presents a large bias, as shown in Table XX, and therefore this has to be quantified precisely in order to provide a value for A^{Δ}, rather than a confidence interval. In addition, improvements on the determination of the acceptance parameters will be essential in order to improve the mea-

Experimental effect	**Uncertainty**
Statistical error	0.28
Gaussian constraint on τ_s and $\Delta\Gamma_s$	0.12
Uncertainty on acceptance parameter	0.42
Resolution	0.06
Experimental effects combined	0.44
Total	0.52

Table 10: Summary of the experimental effect on the sensitivity

Experimental effect	**Bias**
Statistical bias	0.006
Gaussian constraint on τ_s and $\Delta\Gamma_s$	0.008
Uncertainty on acceptance parameter	0.057
Resolution	0.008
Experimental effects combined	0.073
Total	0.79

Table 11: Summary of the experimental effect on the bias

surement, since the imperfect knowledge of their values induces a systematic uncertainty much larger than the statistical one. Finally, let us know that with the current sensitivity it is not expected to be able to rule out any NP models.

As next steps for this study, a few points have to be investigated:

- The bias caused by each of the studied effects, as well as the combined one, needs to be understood as much as possible. Large statistics of toys need to be run in order to determine it precisely.

- Since backgrounds present a peak at very low proper times, it is usual that these are removed from the fit. Therefore, the effect of removing low proper times from the fit should also be studied, and the sensitivities recomputed.

- The presence of background can induce further uncertainties and bias, and therefore it should be added in future works.

As a conclusion the precision measurement of $\mathcal{A}^{\Delta}$ and especially measurements differentiating two potential models is not possible in the current data with the current precision on the parameters. But further studies as well as higher statistics could reduce these uncertainties, and allow precise measurement of $\mathcal{A}^{\Delta}$.

References

[1] F. James, *Statistical Methods in Experimental Physics*, 2nd Edition, CERN Switzerland, 2008

[2] T.M. Karbach, *Feldman-Cousins Confidence Levels - Toy MC Method*, TU Dortmund, Germany, September 6 2011

[3] G. J. Feldman, R.D. Cousins, *A Unified Approach to the Classical Statistical Analysis of Small Signals*, Department of Physics, Havard University, Cambridge, Department of Physics and Astronomy, University of California, Los Angeles, February 2 2008

[4] L. Demortier, L. Lyons, *Everything you always wanted to know about pulls*, The Rockefeller University, University of Oxford, February 26, 2002

[5] J. Beringer et al. (Particle Data Group), PR D86, 010001 (2012) (URL: http://pdg.lbl.gov)

[6] O. Deschamps, M. Hobollah, *Propertime study*, presentation at the Radiative meeting December 16 2013, LHCb

[7] L. Shchutska, et al., *Probing the photon polarization in $B_s \to \phi\gamma$ at LHCb*, LHCb-PHYS-2007-147, December 20, 2007

[8] B. Adeva et al., *Roadmap for selected measurement at LHCb (chapter 7)*, LHCb-PUB-2009-029 (2009), arXiv:0912.4179v3

[9] F. Soomro, *Radiative decays of B mesons at LHCb*, CERN-THESIS-2011-035, Imperial College London, June 17, 2011

[10] A. Puig Navarro, *First measurement of radiative B decays in LHCb*, CERN-THESIS-2012-25, February 2012

[11] The LHCb collaboration, *Measurement of the ratio of branching fractions $\mathcal{B}(B^0 \to K^{*0}\gamma)/\mathcal{B}(B_S^0 \to \phi\gamma)$ and the direct CP asymmetry in $B^0 \to K^{*0}\gamma$*, CERN-PH-EP-2012-247, LHCb-PAPER-2012-019, August 28, 2012

[12] A. del Río Vega, *Estudio de la polarizacíon del fotón en procesos $B_s \to \phi\gamma$ en el experimento LHCb*

[13] D. Atwood, M. Gronau, A. Soni, *Mixing-induced CP Asymmetries in Radiative B Decays in and beyond the Standard Model*, TECHNION-PH-97-11, April 9, 1997

[14] F Muheim, Y. Xie, R. Zwicky, *Exploiting the width difference in $B_s \to \phi\gamma$*, IPPP/08/04, February 6, 2008, University of Edinburgh, University of Durham

[15] F. Soomro, *$B \to X_s\gamma$ and $B \to X_s l^+ l^-$ decays at LHCb*, LHCb-PROC-2011-003, Januray 9, 2011

[16] D. Pirjol, *Probing New Physics with $b \to s\gamma$ decays*, Department of Physics, UCSD

[17] H. E. Haber, G.L. Kane, *The search for Supersymmetry: probing physics beyond the Standard Model*, Phys. Rept. 117 (1985) 75.

[18] R. N. Mohapatra, J. C. Pati, *Left-right gauge symmetry and an "iso-conjugate" model of CP violation*, Phys. Rev. D 11 (1975) 566.

[19] The ALTAS Collaboration, *Observation of a New Particles in the Search for the Standard Model Higgs Boson with the ATLAS Detector at the LHC*, CERN-PH-PH-EP-2012-218, Aug. 31, 2012, arXiv:1207.7214v2

[20] The CMS Collaboration, *Observation of a new boson at a mass of 125 Gev with the CMS experiment at the LHC*, CERN-PH-EP-2012-220, January 28, 2013, arXiv:1207.7235v2

[21] A. Puig,*Photon polarization with the $B \to K_1(1270)\gamma \to (K\pi\pi)\gamma$ decay*, July 23, 2012

A Biased estimator

Let us find the Maximum Likelihood Estimator (MLE) of a simple exponential distribution:

$$f(t) = \Gamma e^{-\Gamma t} \tag{24}$$

The aim is to compute the bias of such an estimator.

A.1 Maximum Likelihood

The likelihood of distribution described in Eq. 24 is:

$$L = \prod_{i=1}^{N} f(t_i) = \prod_{i=1}^{N} \left(\Gamma e^{\Gamma t_i}\right) = \Gamma^N \exp\left(-\sum_{i=1}^{N} \Gamma t_i\right) \tag{25}$$

Thus:

$$\ln L = N \ln \Gamma - \sum_{i=1}^{N} \Gamma t_i \tag{26}$$

A.2 MLE

As the MLE $\hat{\Gamma}$ maximizes the likelihood:

$$\frac{\partial \ln L}{\partial \Gamma}(\hat{\Gamma}) = 0 \iff \hat{\Gamma} = \frac{N}{\sum_{i=1}^{N} t_i} = \frac{1}{\bar{T}} \tag{27}$$

A.3 Bias

In order to compute the bias of the MLE $\hat{\Gamma}$ we need to the compute the expectation value of $\hat{\Gamma}$. We know that:

$$\mathbb{E}(\hat{\Gamma}) = \mathbb{E}(\frac{1}{\bar{T}}) = \int \frac{1}{\bar{T}} f(\bar{T}) d\bar{T} \tag{28}$$

Where $f(\bar{T})$ the distribution function of the mean $\bar{T}$ is. In order to find an expression for $f(\bar{T})$ we need to use the moment generating functions:

$$M_{\bar{T}} = \mathbb{E}(\exp(x\bar{T})) \tag{29}$$

$$= \mathbb{E}(\exp(xN^{-1} \sum_{i=1}^{N} t_i)) \tag{30}$$

$$= \mathbb{E}(\prod_{i=1}^{N} \exp(xN^{-1} t_i)) \tag{31}$$

But we also have by definition of the exponential distribution, that:

$$M_{t_i}(x) = \mathbb{E}(\exp(xt_i)) = \left(1 - \frac{x}{\Gamma}\right)^{-1} \tag{32}$$

Hence:

$$M_{\bar{T}}(x) = \prod_{i=1}^{N} \mathbb{E}(\exp(xN^{-1} t_i)) \tag{33}$$

$$= \prod_{i=1}^{N} M_{t_i}(xN^{-1}) \tag{34}$$

$$= \left(1 - \frac{x}{N\Gamma}\right)^{-N} \tag{35}$$

We can identify this as the moment generating function of the Gamma distribution with shape parameter N and inverse scale parameter $N\Gamma$, which in terms gives us the distribution function of the mean $\bar{T}$:

$$f(\bar{T}) = \Gamma(N, N\Gamma)(\bar{T}) \tag{36}$$

Therefore:

$$\mathbb{E}(\hat{\Gamma}) = \int \frac{1}{\bar{T}} f(\bar{T}) d\bar{T} \tag{37}$$

$$= \int \frac{1}{\bar{T}} \frac{(N\Gamma)^N)}{\Gamma(N)} \bar{T}^{N-1} e^{-N\Gamma\bar{T}} d\bar{T} \quad = \frac{1}{\Gamma(N)} N\Gamma \int u^{N-2} e^{-u} du \tag{38}$$

where we used the change of variables : $u = N\Gamma\bar{T}$. We can now identify the Gamma function $\Gamma t = \int x^{t-1} e^{-x} dx$ to get:

$$\mathbb{E}(\hat{\Gamma}) = N\Gamma \frac{\Gamma(N-1)}{\Gamma(N)} \tag{39}$$

Which finally gives:

$$\mathbb{E}(\hat{\Gamma}) = \frac{N\Gamma}{N-1} \tag{40}$$

We can now compute the bias:

$$b_{\hat{\Gamma}} = \frac{\Gamma}{N-1} \tag{41}$$

The MLE $\hat{\Gamma}$ is thus biased but consistent as it vanishes for high number of events meaning high values of N.

B Results

B.1 PureToy

Table 12: Confidence levels used to construct the Confidence Belt for pure toys

$\mathcal{A}^{\Delta}$	**Lower Limit**	**Upper Limit**
	1σ	
-0.45	-0.791173	-0.124719
-0.4	-0.744063	-0.0800875
-0.35	-0.688571	-0.0322762
-0.3	-0.63199	0.0187973
-0.25	-0.581778	0.064729
-0.2	-0.524497	0.110656
-0.15	-0.47799	0.158455
-0.1	-0.421406	0.209055
-0.05	-0.372819	0.252692
0.0	-0.31785	0.302745
0.045	-0.274597	0.344148
0.05	-0.268389	0.348157
0.1	-0.210855	0.396364
0.15	-0.16055	0.444389
0.2	-0.111549	0.493369
0.25	-0.0540299	0.540934
0.3	0.00135434	0.583187
0.35	0.0548613	0.632477
0.4	0.104163	0.681652
0.45	0.153985	0.724599
0.5	0.206379	0.774433
0.55	0.262289	0.820783
0.6	0.311964	0.870174
0.65	0.367991	0.91833
0.67	0.383356	0.935035
0.7	0.422404	0.965157
0.75	0.473249	1.01105
0.8	0.522632	1.06154
0.85	0.580095	1.11101
0.9	0.632768	1.15574
0.95	0.683534	1.20402
1.0	0.735878	1.24762
	2σ	
-0.45	-1.1516	0.188106
-0.4	-1.09976	0.228187
-0.35	-1.04297	0.282745
-0.3	-0.982413	0.31916
-0.25	-0.924046	0.362629
-0.2	-0.876719	0.410911
-0.15	-0.820229	0.45266
-0.1	-0.766947	0.506099
-0.05	-0.707688	0.543333
0.0	-0.652862	0.593821
0.045	-0.604994	0.626488
0.05	-0.598028	0.635064
0.1	-0.538753	0.675685
0.15	-0.487217	0.72871
0.2	-0.425422	0.767295
0.25	-0.371344	0.812917
0.3	-0.318654	0.856648
0.35	-0.256163	0.904623
0.4	-0.203124	0.946555
0.45	-0.152072	0.994344
0.5	-0.0981446	1.03796
0.55	-0.0337128	1.08328
0.6	0.0125602	1.12898
0.65	0.0692354	1.17516
0.67	0.0916025	1.18966
0.7	0.132219	1.21773
0.75	0.185333	1.26094
0.8	0.235875	1.30874
0.85	0.29727	1.34918
0.9	0.339513	1.39523
0.95	0.406577	1.44755
1.0	0.465525	1.48418
	3σ	
-0.45	-1.52563	0.48733
-0.4	-1.46139	0.518676
-0.35	-1.43018	0.584641
-0.3	-1.34535	0.600751

-0.25	-1.30434	0.654191
-0.2	-1.23471	0.693843
-0.15	-1.18048	0.734857
-0.1	-1.11855	0.784957
-0.05	-1.05519	0.81502
0.0	-1.00984	0.868421
0.045	-0.929385	0.890807
0.05	-0.933771	0.897554
0.1	-0.897013	0.948934
0.15	-0.844131	0.988834
0.2	-0.779242	1.01839
0.25	-0.711323	1.07923
0.3	-0.621207	1.10684
0.35	-0.589402	1.15455
0.4	-0.526306	1.20616
0.45	-0.478879	1.25371
0.5	-0.420237	1.30735
0.55	-0.34647	1.32901
0.6	-0.296993	1.37256
0.65	-0.250485	1.41626
0.67	-0.221369	1.44958
0.7	-0.200956	1.45955
0.75	-0.113448	1.49997
0.8	-0.0607708	1.551
0.85	-0.000440126	1.59231
0.9	0.0462583	1.62983
0.95	0.115294	1.68631
1.0	0.171034	1.71591

B.2 All effect combined

Table 13: Confidence levels used to construct the Confidence Belt for toys containing all the experimental effect : acceptance, resolution and uncertainties on B mesons parameters and acceptance parameters

$\mathcal{A}^{\Delta}$	**Lower Limit**	**Upper Limit**
	1σ	
-0.45	-1.12527	0.0842193
-0.4	-1.04708	0.133212
-0.35	-0.984523	0.175481
-0.3	-0.936026	0.208137
-0.25	-0.873133	0.263188
-0.2	-0.820474	0.305878
-0.15	-0.765271	0.344272
-0.1	-0.702931	0.384399
-0.05	-0.644911	0.426223
0.0	-0.583225	0.464542
0.045	-0.536215	0.510736
0.05	-0.526123	0.511527
0.1	-0.476868	0.561879
0.15	-0.412967	0.604655
0.2	-0.348254	0.643717
0.25	-0.296648	0.685576
0.3	-0.235078	0.730696
0.35	-0.186064	0.767318
0.4	-0.124129	0.813274
0.45	-0.0673762	0.863823
0.5	-0.00754212	0.908261
0.55	0.0526023	0.950274
0.6	0.109908	0.990122
0.65	0.159276	1.03384
0.67	0.186232	1.05182
0.7	0.223893	1.08916
0.75	0.281455	1.12582
0.8	0.334743	1.17802
0.85	0.393449	1.21728
0.9	0.451086	1.26366
0.95	0.500609	1.30562
1.0	0.560152	1.34997
	2σ	
-0.45	-1.9136	0.548576
-0.4	-1.83745	0.58636
-0.35	-1.77205	0.633096
-0.3	-1.70574	0.655401
-0.25	-1.63406	0.699455
-0.2	-1.57482	0.729552
-0.15	-1.49818	0.771802
-0.1	-1.42433	0.813059

-0.05	-1.35207	0.831798
0.0	-1.29201	0.875431
0.045	-1.23083	0.913409
0.05	-1.21789	0.916704
0.1	-1.15256	0.955191
0.15	-1.07143	0.993746
0.2	-0.999234	1.02604
0.25	-0.957948	1.07458
0.3	-0.862831	1.09769
0.35	-0.828138	1.137
0.4	-0.742417	1.18225
0.45	-0.69451	1.2154
0.5	-0.598998	1.25169
0.55	-0.545846	1.29776
0.6	-0.47975	1.33195
0.65	-0.409189	1.37492
0.67	-0.399568	1.38406
0.7	-0.343644	1.4241
0.75	-0.264898	1.45694
0.8	-0.215217	1.50799
0.85	-0.15297	1.53673
0.9	-0.0876865	1.58163
0.95	-0.0334058	1.61646
1.0	0.0440347	1.64713
	3σ	
-0.45	-2.9071	0.937341
-0.4	-2.79644	0.96574
-0.35	-2.72985	1.02686
-0.3	-2.73548	1.02985
-0.25	-2.60805	1.07485
-0.2	-2.45317	1.10156
-0.15	-2.46521	1.12808
-0.1	-2.32347	1.18944
-0.05	-2.20481	1.20618
0.0	-2.17542	1.20414
0.045	-2.14691	1.25568
0.05	-2.08754	1.26259
0.1	-2.0602	1.29808
0.15	-1.87954	1.33295
0.2	-1.85688	1.3257
0.25	-1.7943	1.38578
0.3	-1.66442	1.44537
0.35	-1.60641	1.45803
0.4	-1.51029	1.48142
0.45	-1.49268	1.50996
0.5	-1.31447	1.54742
0.55	-1.32769	1.59698
0.6	-1.21469	1.61396
0.65	-1.10009	1.66352
0.67	-1.12526	1.69008
0.7	-1.04144	1.70321
0.75	-0.976813	1.73012
0.8	-0.911834	1.78297
0.85	-0.859111	1.81414
0.9	-0.767777	1.85543
0.95	-0.702917	1.88745
1.0	-0.565922	1.92865